This is to certify that the

thesis entitled

TEXTURE CHANGE IN PASTRIES AS A FUNCTION OF PACKAGING AND STORAGE ENVIRONMENT

presented by

DAVID SCOTT STALEY

has been accepted towards fulfillment
of the requirements for

M.S. degree in Food Science

Dennis R. Heldman
Major professor

Date 9/30/85

TEXTURE CHANGE IN PASTRIES AS A FUNCTION OF PACKAGING AND STORAGE ENVIRONMENT

By

David Scott Staley

A THESIS

Submitted to
Michigan State University
in partial fulfilment of the requirements
for the degree of

MASTER OF SCIENCE

Department of Food Science and Human Nutrition

1985

ABSTRACT

Texture Change in Pastries as a Function of Packaging and Storage Environment

By

David Scott Staley

Shelf-life determinations of foods normally involve expensive, time-consuming experiments. This research develops mathematical relationships describing texture change as a function of water activity and temperature.

Pastries were brought to water activities of 0.20, 0.30, 0.45, 0.60 and 0.75, packaged in foil pouches, and stored at 10, 20, 32, and 43 C. Hardness, cohesiveness, and bending values were measured during storage. Hardness was the most sensitive test. Initial hardness was described by an inverse linear relationship with water activity. First order rate constants of hardness change as a function of water activity were described by an exponential relationship while temperature dependence was described by an Arrhenius relationship. These and other relationships were used in a computer program to predict hardness and moisture content of pastries packaged in polyethylene, polystyrene, and foil pouches stored at temperatures from 11 C to 40 C and relative humidities between 35 %RH and 62 %RH.

David Scott Staley

Approved: Dennis R. Heldman

Date: Oct 1, 1985

ACKNOWLEDGMENTS

The author would like to express his gratitude to Dr. Dennis R. Heldman for his technical assistance and guidance throughout the Masters Degree program. The author is also indebted to Dr. Heldman for providing a graduate assistantship and a challenging environment to study in.

Appreciation is extended to Dr. Bruce Harte, Dr. James Steffe, and Dr. Mary Zabik for serving on the author's guidance committee.

Grateful acknowledgment is given to the author's parents, Loren and Joyce Staley, who taught the author to value greatly the pursuit of knowledge and aided him in obtaining a higher education.

Most of all, the author wishes to express his deepest appreciation and love to his wife, Mary, and his brother, Eric, for their perservering assistance in performing experiments and in the final preparation of this study. Their enthusiastic encouragement, constant availability, and unselfish aid were largely responsible for the eventual success of this work.

TABLE OF CONTENTS

page

page

LIST OF TABLES

page

LIST OF FIGURES

NOMENCLATURE

a = Smith constant, monolayer moisture

a_w = water activity of sample

$a_{w,o}$ = outside water activity (RH/100)

A = Area, m^2

A_1 = area under TPA curve #1

A_2 = area under TPA curve #2

b = Smith constant, slope of curve in multilayer fraction

B = bending value, N/m

B_o = bending value at time zero

c = concentration

C = cohesiveness

C_o = cohesiveness at time zero

da_w = change in water activity

dm = change in dry basis moisture content, kg H_2O/kg solids

dt = time increment, hours

D = diffusion coefficient, kg/(m s)

D_t = display increment, days

E.R.H. = equilibrium relative humidity (E.R.H./100 = a_w), %

E = activation energy, kJ/mol

f = flux, kg/(m^2s)

F = force applied, N

H = hardness, N

H_o = hardness at time zero

k = kinetic rate constant, 1/s

k_B = kinetic rate constant for change in bending value, 1/s

k_C = kinetic rate constant for change in cohesiveness, 1/s

k_H = kinetic rate constant for change in hardness, 1/s

k_o = Arrhenius constant for change in texture

K_a = intercept of rate constant vs. a_w curve

K_b = slope of rate constant vs. a_w curve

ℓ = package film thickness, m

L = pastry thickness, m

m = dry basis moisture fraction, kg H_2O/kg solids

m_o = initial dry basis moisture fraction, kg H_2O/kg solids

M = dry basis moisture percent, kg H_2O/100kg solids

M_a = intercept of texture vs. a_w curve

M_b = slope of texture vs. a_w curve

M_o = initial dry basis moisture percent, kg H_2O/100kg solids

n = order of change

p = vapor pressure, Pa

p_s = saturation vapor pressure, Pa

P = package film permeability constant, kg m/(m^2 s Pa)

P_o = Arrhenius constant for permeability constant

R = gas constant, J/(mol K)

RH = relative humidity, %

S = solubility coefficient, 1/Pa

S_t = storage time, days

t = time, s

T = temperature, C

T_a = absolute temperature, K

T_r = reference temperature, C

TPA = texture profile analysis

$\mathcal{T}$ = texture

$\mathcal{T}_o$ = initial texture

V = concentration or other variable

w_p = product mass, kg

w_s = solids mass of product, kg

x = distance of permeation, m

I. INTRODUCTION

The development of low and intermediate moisture foods is often affected by factors involving the measurement of food texture. It is often necessary to establish the storage life of a food product based on its perceived texture due to moisture uptake or physiochemical change. But the determination of shelf-life of a product normally involves time consuming, costly experiments. The potential interaction of variable environmental and processing factors adds to the complexity of these types of studies. Changing either the environment or type of package can seriously alter the outcome, sometimes requiring repetition of the shelf-life study. Therefore, a computer simulation of texture which is more efficient, less expensive and yet effective would serve as an alternative approach or back up to shelf-life tests. As an added benefit, computer simulations can be helpful to the packaging engineer in the selection of an optimum package system, or to Quality Control personnel to identify the status of product quality in different climates.

The development of an effective computer simulation requires knowledge of the direct effect of moisture uptake on texture as well as experimental kinetic data of texture

change as a function of water activity and temperature. In addition, moisture transfer properties of the packaging material and the physical dimensions of the package are required. One must also select a suitable texture measurement that adequately represents the textural characteristics that affect the product quality.

At one time, research work on texture implied that texture could be characterized by one parameter. It is now generally accepted that texture is described by several different parameters. Acceptable texture data may be obtained from subjective sensory human panels or from objective mechanical measurements. In general mechanical measurements require less time and resources to obtain though identifying one objective texture measurement to describe a product's textural qualities is difficult and selection of a method can be a subjective exercise.

In this study, three parameters were utilized to describe texture. Two parameters were identified from the General Foods Texture Profile Analysis adapted for the Instron Universal Testing Machine; hardness and cohesiveness. The third parameter was obtained from the same machine by measuring the bending force needed to break the pastry.

The overall objective of this investigation was to select a suitable texture measurement then develop and verify a computer model to predict the texture change in a pastry-type food. More specifically the objectives are:

1) to determine the effect of product water activity on initial pastry texture,

2) to determine the relationship between the rate of texture change and product water activity based on experimental kinetic data,

3) to incorporate mathematical relationships describing the rate of texture change as functions of water activity and temperature into a computer program developed to predict pastry texture during storage and,

4) to verify the computer prediction model using experimental shelf-life data.

II. REVIEW OF LITERATURE

2.1 Texture Measurement

The problem of defining texture as a major component of food quality arose as a gradual awareness developed that sensory quality of foods does not consist of a single well-defined attribute but is a composite of many. Smith (1947a) was among the first to list more specific properties of food quality as nine distinct parameters contributing to overall quality (size, viscosity, thickness, texture, consistency, turbidity, color, succulence, and flavor). Kramer (1955) pointed out that sensory quality of foods is a psychological as well as physical phenomenon and should be systemized or classified in accordance with the senses; appearance (sight), flavor (taste), olfactory (smell), and kinesthetics or texture (touch). Sound was thought to be of minor importance in classification of food quality. There was reluctance on the part of some workers however, to assign a primary role to the term texture in sensory evaluation due to its use in describing many different sensations such as hardness, viscosity, mouthfeel, graininess, etc. Its precise meaning was not evident. Kramer (1964) proposed limiting texture further to the sense of feel only and from

a physical standpoint to the part of rheology that deals with the deformation and flow of matter, but only as a result of the application of force greater than gravity. Other parameters of texture were further classified in accordance with how the force is applied to cause specific types of deformation such as compression, shearing, etc. Since then, a number of additional textural classifications were proposed. Szczesniak (1963b) and Bourne (1966a,b) dealt with solid products mainly while Sherman (1969) utilized the state (solid vs. fluid) of the product in a classification of masticatory properties. Mohsenin (1970a,b) defined mechanical properties of solid foods in rheological terms, providing more understanding of mechanical properties that could be related to human responses.

Texture is a sensory property of food and may be measured in a subjective way with the human senses. More objective measurements can be obtained however by rheological methods. Although objective measurements of texture have the disadvantage of measuring sensory properties indirectly and are accurate only to the extent that they resemble human sensory responses, they are objective and are not subject to change or fatigue and are more reliably consistent than the human senses (Szczesniak,1973).

Szczesniak (1973) classified instrumental methods of texture measurement as: 1) a probe contacting a food sample, 2) a driving mechanism providing force, 3) a sensing element

for detecting the resistance of the foodstuff to the force, and 4) a readout system. Szczesniak (1973) further classified texture measuring devices as 1) penetrometers; 2) compressimeters, 3) shearing devices, 4) cutting devices, 5) masticometers, 6) consistometers 7) viscometers, 8) extrusion measurements, and 9) multi-purpose units. Indirect methods of texture measurement were classified as 1) chemical, 2) enzymatic, 3) microscopic, and 4) physical.

Multi-purpose units can be used to measure a number of different texture tests, and are used extensively because of their versatility, flexibility, and accuracy (Szczesniak,1973). Popularly used machines include the Instron Universal Testing Machine and Food Technology Corporation's Texture-Testing System (widely known as the Kramer Shear Press when referring to a particular test probe that uses a number of metal plates to shear the sample). The Instron is an especially versatile unit. The Instron is composed of a mechanical drive system, a load cell to measure forces of compression or tension, a recorder, and an array of controls. The unit allows for precise knowledge of force exerted and distance covered by the test probe into the sample. A number of test probes can be incorporated into the Instron.

The realization that texture is composed of a number of different parameters however, complicates the search for a suitable texture measurement that adequately represents the textural characteristics influencing the product quality.

It was with these problems in mind that the General Foods Texture Profile Analysis (TPA) was devised. It is based on a set of textural characteristics which combine fundamental rheological principles and common nomenclature used to describe texture. It also lends itself to applied research and a vast variety of food products (Szczesniak,1963a). Originally designed to be used with the General Foods Texturometer, the Texture Profile Analysis was later adapted to the Instron Universal Testing Machine by Bourne (1968). Mechanical characteristics for the Texture Profile Analysis were divided into five primary parameters; hardness, cohesiveness, elasticity (now referred to as springiness), adhesiveness and into three secondary parameters: brittleness (now referred to as fracturability), chewiness, and gumminess. The secondary parameters are values that further describe the characteristics of hardness and cohesiveness. The cyclic nature in applying force and the similarity to the masticatory process may have contributed to the good correlations found between Texturometer readings and human panel results (Friedman et al.,1963)

2.2 Influence of Water Activity and Moisture on Texture

There are few published reports concerning the effects of moisture adsorption on texture. Lakhanpal and Flood (1957) and Flood and Farhan (1963) proposed a thermodynamic theory of adsorption-extension phenomenon based on tensile stresses observed, caused by the adsorption of gases and

vapor by activated carbon. Lundgren (1967) studied the flex-fatigue life of wool fibers at various moisture contents and temperatures. Bettelheim and Ehrlich (1963) investigated the thermodynamics and other aspects of water vapor sorption by mucopolysaccharides, including hypotheses based on structural alterations of the components. Masuzawa and Sterling (1968) reported that in hydrophilic polymers, differences in the standard differential entropy and enthalpy values with sorbed water were related to differences in the strength of intermolecular associations as affected by steric hindrance. Kapsalis et al. (1970a) revealed certain relationships between water sorption and the textural properties of freeze-dried foods. A Masticometer was used to determine texture at increasing penetration depths of various food materials over a water activity range of 0.0 to 0.66. The foods were tested after storage but texture was not monitored during storage. Later Kapsalis et al. (1970b) studied the relationships between water activity and textural properties over a water activity range of 0.0 to 1.0. Two instruments were used to measure texture of freeze-dried meat samples. The Allo Kramer Shear Press was used for shear measurements involving cutting and extrusion. An Instron Universal Testing Machine was used for compression measurements. In the cutting-extrusion experiments, maximums in the force vs. water activity curves were observed at a water activity of 0.85. In the compression experiments, significant textural changes were

observed in the 0.15 to 0.30 water activity range. These changes were correlated with changes in the standard differential entropy of the freeze-dried beef.

Reidy and Heldman (1972) used the Texture Profile Analysis adapted for the Instron Universal Testing Machine to measure hardness and chewiness of freeze-dried beef cubes at various water activities. All measurements were made immediately after equilibration and products were not stored for any length of time. Reidy and Heldman (1972) found hardness and chewiness to be relatively constant in the 0.0 to 0.6 water activity range but decreased significantly at higher water activities. Maximum values were found near a water activity of 0.4. Later, Reidy and Heldman (1974) were able to predict texture profile for freeze-dried foods using engineering parameters. A four-parameter mathematical model was used to describe the response of freeze-dried beef to cyclic loading over the water activity range of 0.15 to 0.92. In general, parameters of the mathematical model and corresponding texture paramaters (hardness and chewiness) decreased with increasing water activity. There was a tendency for parameters of the mathematical model to attain maximum values at intermediate water activities.

Similar experiments were performed on Sugar-Snap cookies by Zabik, Fierke, and Bristol (1979) with measurements taken after equilibration. Water activities of the cookies ranged from 0.11 to 0.93. Crispness was determined as breaking strength using a single blade cell

and tenderness using the standard shear compression cell with an Allo Kramer Shear Press. Breaking strength and compressibility were determined with the Instron Universal Testing Machine. Breaking strength was found to be the most sensitive test involving a linear relationship with water activity.

2.3 Reaction Kinetics in Foods

Time dependence of chemical reactions in foods are usually described by classical reaction kinetics which refer to zero, first, and second order equations. Data may be fit to these equations in a number of ways using a variety of statistical procedures (Labuza and Kamman, 1983; Lund, 1982). For many physical changes in foods, it is difficult to distinguish between zero, first, and second order processes. For processes in which a physical property does not change by more than 50%, analytical precision greater than 5% is needed to distinguish between zero, first, and second order kinetics (Lund,1983). This level is very difficult to obtain because of the biological heterogeneity in food materials. Many second order reactions are pseudo-first order, and can be modeled as first order because one reactant is present at concentrations in excess of the other. It is for these reasons that many physical changes and chemical reactions can be modeled as a first order process (Lund,1983). This is especially useful on occasions

where the specific reactions causing physical changes are unknown.

With respect to texture, many dehydrated and intermediate moisture foods become tough during storage. Protein denaturation and starch retrogradation may be causing texture change. Two reaction mechanisms causing protein denaturation have been cited to explain this increase in hardness; lipid oxidation and non-enzymatic browning (Labuza,1974).

With lipid oxidation, oxygen will react with unsaturated fats yielding free radicals and peroxides. These radicals and peroxides can react with proteins producing crosslinkages causing the protein matrix to become insolubilized which leads to toughening of the product. With increasing water activities, the rate of oxidation increases and reaches a maximum at higher water activities. The amount of water may not be critical in the reaction (Labuza,1974).

Non-enzymatic browning refers to the deteriorative Maillard reactions where reducing sugars react with amino acids and proteins to produce brown pigmented polymers. A loss in solubility causes irreversible aggregation of the polymers resulting in toughening of the food (Labuza,1974).

Starch retrogradation may also play an important role in texture change. Intermolecular association of starch molecules may be caused by the formation of crystal nuclei on which additional segments of starch molecules may be

layered to form crystalline regions. As increasingly longer portions of molecules pull together by intermolecular association, the starch matrix shrinks and water is forced out. This increased association of starch molecules for each other is known as retrogradation (Paul and Palmer,1972). A return to a more orderly, partially crystalline state by an accompanying loss of water holding capacity may result in toughening of a food product.

The above mechanisms have been found to follow first order kinetics in the case of lipid oxidation (Fritsch and Gale,1977) and starch retrogradation (Meisner,1953) or have been designated as zero order (Hendel,Silveira,and Harrington,1955) but can be modeled as first order in the case of nonenzymatic browning.

2.3.1 Influence of Temperature on Kinetic Rate Constants

Similar to other qualitative determinations, the Arrhenius equation has been used to describe the temperature dependency of reaction kinetics for many chemical reactions in foods. Ragnarsson and Labuza (1977), Ragnarsson et al (1977), and Labuza and Bergquist (1983) have used the Arrhenius equation to describe the influence of temperature on lipid oxidation. Hendel, Silveira, and Harrington (1955) used Arrhenius type plots to characterize the effect of temperature on nonenzymatic browning in dehydrated potato. Meisner (1953), Pence and Standbridge (1955), Axford et al.. (1968); and Kim and D'Appolonia (1977a,b) showed temperature

dependency of starch retrogradation in bread with Arrhenius plots. The results from each of these researchers reflect the negative activation energies characteristic of starch retrogradation. As temperature increases the rate of retrogradation decreases. From a functional standpoint however, Kulp and Lorenz (1984) have shown from microscopic analysis that starch does not gelatinize during the baking process in cookies and other low moisture, high fat pastries (as opposed to breads) and cannot participate in staling by retrogradation. In this study therefore, negative activation energies for texture change are not to be expected as a result of starch retrogradation. For typical activation energies (E) obtained for the above reactions, see Table 2.1.

2.3.2 Influence of Water Activity on Kinetic Rate Constants

Water is not only the most abundant component in foods but plays an extremely important role in the general acceptability of many foods. In addition, water is resonsible for food's perishable nature, and governs the rates of many chemical reactions. With respect to chemical reactions, water acts as solvent for chemical species to diffuse and react with each other. The control of moisture is very important in dry and intermediate moisture foods too. Water does not have to be available as a solvent however, to affect rates of chemical deterioration (Labuza,1974). It is now generally known that food quality

Table 2.1 - Typical activation energies of nonenzymatic browning, lipid oxidation, and starch retrogradation

Reaction	Source	E, kJ/mol
lipid oxidation	Fritsch and Gale (1977)	61 - 82
	Labuza and Bergquist (1983)	84 - 92
	Labuza (1971)	42 - 101
nonenzymatic browning	Labuza (1974)	105 - 113
	Hendel et al. (1955)	105 - 155
starch retrogradation	Meisner (1953)	-27.6
	Pence and Standbridge (1955)	-50.2
	Axford et al. (1968)	-36.0
	Kim and D'Appolonia (1977a,b)	-40.2

is not affected so much by the actual amount of water present as by the physicochemical state in which water exists.

Water activity, the availability of water for chemical reaction, is determined by the water vapor pressure in a system relative to that of pure water. Figure 2.1 (Labuza,1971) shows the relative rates of common deteriorative reactions in food as a function of water activity.

2.4 Influence of the Semipermeable Package on Moisture Transfer

The protection of foods from the environment greatly depends on the permeability of the packaging material used as well as the package integrity including seals, seams and closures. Gases can permeate through packaging films by macroscopic or microscopic pores and pinholes or by diffusion through the material itself (Ayer et al.,1960). In diffusion, a gas will dissolve in the packaging material at one surface, diffuse through the material as a result of a concentration gradient, and evaporate from the other surface.

The permeability coefficient, as defined by Hauser and McLaren (1948), of many packaging films to water vapor increases with higher relative humidities. This may be due to the sorption of water producing a plasticizing effect on the film allowing higher rates of vapor transmission. This

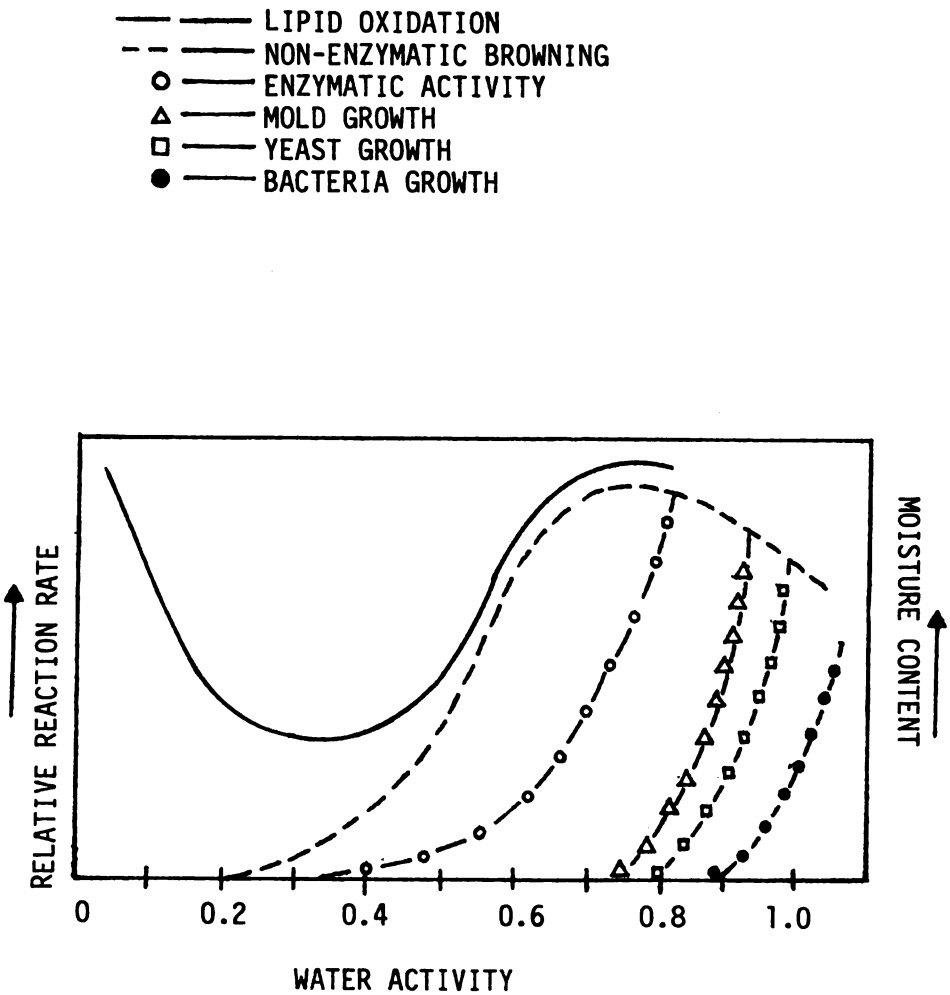

Figure 2.1 Relative reaction rates of foods as a function of water activity (Labuza, 1971)

is true for hydrophilic polymers such as nylon, cellulose, and polyvinyl alcohol. For rubbers, this dependence is less pronounced and may either increase or decrease with relative humidity (Taylor et al., 1936; Rowan, 1956; Ayer et al., 1960).

Temperature is another factor that influences the permeability constant. Generally, the permeability constant increases with temperature. Barrer (1941) indicates that the least permeable membranes are more sensitive to temperature changes than others. In many cases this temperature dependence can be characterized by an Arrhenius relationship (Doty et al., 1946; Myers et al., 1961).

2.5 Computer Simulation of Quality Change in Low and Intermediate Moisture Foods

A number of computer simulations to predict the shelf-life of food products have been developed. Most of these programs require knowledge of the kinetics of the limiting deteriorative mechanism and depend on the mass transfer properties of the packaging materials (Labuza et al., 1972; Purwadaria, Heldman, Kirk 1979).

Prediction of shelf-life of oxidation-sensitive foods has been the subject of a number of these studies. Simon et al. (1971) developed a computer prediction model describing the oxidative deterioration of freeze-dried shrimp. Organoleptic deterioration was correlated with oxygen uptake and with loss of carotenoid pigment. Kwolek and Bookwalter

(1971) presented a model which determined storage stability as a function of time, temperature, and kinetics of oxidative rancidity. The model utilized flavor and peroxide value data previously published by Bookwalter et al. (1968). Quast et al. (1972a,b) developed a mathematical model for the oxidation of potato chips as a function of oxygen partial pressure, equilibrium relative humidity, and degree of oxidation. Later, Quast and Karel (1972) presented a computer simulation for potato chips which undergo deterioration by two mechanisms simultaneously: loss of crispness due to moisture adsorption and lipid deterioration because of exposure to atmospheric oxygen. Quast and Karel (1973) then used the computer simulation to determine the optimum packaging film permeability to minimize the deterioration of the two interaction mechanisms of moisture uptake and oxidation.

Mizrahi et al. (1970) characterized nonenzymatic browning with a computer model for freeze-dried cabbage stored in different packaging materials. Later, Mizrahi and Karel (1978) demonstrated how the kinetic model for the same reaction can be evaluated using data obtained under conditions of continuously changing moisture content and temperature.

III. THEORETICAL CONSIDERATIONS

3.1 Texture Measurements

The rheological behavior of a system describes the manner in which the system will exhibit flow and/or deformation responses as a result of an applied force. Due to the complex heterogeneous nature of biological materials, it is difficult to measure mechanical properties that adequately describe fundamental stress and strain relationships. Consequently, empirical approaches are used to describe the rheological behavior commonly referred to as texture.

In this study, all measurements involved the use of the Instron Universal Testing Machine. When measuring texture, it was important to keep machine operating conditions consistent between measurements of the same test. This continuity was necessary to compare results effectively. For example, crosshead speed and probe size were kept constant. Variations in sample size were kept to a minimum.

Due to difficulty in maintaining complete control of sample uniformity, numerical and procedural factors were used to compensate for very small variations in sample size. In the case of the hardness and cohesiveness measurements,

sample thickness was measured and penetration depth of the probe was set at ten percent deformation of the sample thickness. For the bending test, the bending value was defined as the breaking or yield force divided by the sample thickness to provide a breaking force per unit depth of pastry (Bruns and Bourne,1975).

3.2 Sorption Isotherms

There have been numerous attempts to describe sorption isotherms by mathematical relationships. Most isotherm equations however, are only accurate over a limited water activity range or are effective for a small class of materials.

The isotherm model used in this research is based on the popular Smith (1947b) equation. The model is based on the theory that two fractions of water are sorbed onto a dry surface. The first fraction exhibits a higher than normal heat of condensation and the second fraction shows a normal heat of condensation. Smith (1947b) expected the first fraction to follow the Langmuir (1918) model which assumes a stoichiometric relationship between the quantity of sorbed water molecules and the number of sorbent binding sites. The latter model has been found to be valid only in the very low water activity range below 0.20 (Kuntz and Kauzmann, 1974). Smith (1947b) based his model on the second fraction which can form only after the first fraction has been sorbed. The second fraction was assumed to consist of

multiple layers of condensed water molecules which effectively block any possible evaporation of the initial layer. Smith (1947b) theorized that moisture content in the second fraction was proportional to the logarithm of the difference between the water activity of the sample and that of pure water. The Smith equation is as follows:

$$M = a + b \ln(1 - a_w) \qquad (3.1)$$

where:

a = the intercept on the moisture content axis representing the quantity of water in the first sorbed fraction or monolayer moisture

b = the slope of the isotherm within the multilayer moisture fraction range

Smith (1947b) justified his theory with sorption data for boiled cotton, nylon, wool, and cellophane. By plotting these data as $-\ln(1-a_w)$ against dry basis moisture content, a curve was obtained at low water activities but the relationship became linear at a water activity of 0.40. The applicability of this model to a wide variety of food materials has been shown by Becker and Salloms (1956), Young (1976), Chirife et al. (1979), and Lang and Steinberg (1980). Lang and Steinberg (1981) found linearization of the water sorption isotherm for homogeneous ingredients over a 0.30 to 0.95 water activity range.

3.3 Influence of Water Activity on Texture

The function of water as a solvent and plasticizer is well known. It is obvious that sauces and doughs are easily thinned and softened by the addition of water. Textural properties of low and intermediate moisture foods are influenced by moisture content as well. But at lower moisture contents, the physiochemical state of the water (i.e. water activity) may be more important than the actual moisture content when considering the food's textural characteristics. Textural properties also depend on conditions and methods of testing which should be carefully specified. Some texture measurements may be sensitive to some aspects of food quality more than others and may be influenced by water activity in a different manner. It is important then, to select the textural measurements that adequately describe the important textural qualities of the product.

Kapsalis, Walker, and Wolf (1970) found that for freeze-dried beef cutting-extrusion forces with the Allo-Kramer Shear Press increased with the square of percent moisture in the 0.0 to 0.85 water activity range. At water activities of 0.15 and 0.30, maximum values were reached for the secant modulus, degree of elasticity, toughness, bioyield strength and work ratio of the second to the first loading cycles measured with the Instron Universal Testing apparatus. A minimum value was reached for the crushability index. Within the same range of 0.15 to 0.85, minima and

maxima were found in the thermodynamic curves, especially the standard differential of entropy for freeze-dried beef. Zabik, Fierke, and Bristol (1979) found crispness and tenderness of Sugar Snap Cookies to vary linearly with water activity as measured with the Allo Kramer Shear Press. Limited correlation was found between water activity and compressibility with the Instron Universal Testing machine. Linearity was observed between water activity and breaking strength as measured by the Instron.

Since there are no definite theoretical relationships to adequately describe the relationships between texture and water activity however, it is more important to select a simple mathematical relationship that adequately describes the phenomena.

3.4 Kinetics of Texture Measurement

Time dependence of chemical reactions of foods is usually described by classical kinetic equations where:

$$\frac{dV}{dt} = kV^n \tag{3.2}$$

where:

V = concentration or other variable

t = time, s

k = rate constant, 1/s

n = the order of change

Texture change may be described by first order kinetics if V is replaced by the texture variable, $\mathcal{T}$, and n = 1 to give:

$$\frac{d\mathcal{T}}{dt} = k \tag{3.3}$$

or upon integration and rearrangement:

$$\mathcal{T} = \mathcal{T}_o \exp(kt) \tag{3.4}$$

where:

$\mathcal{T}_o$ = initial texture

3.4.1 Influence of Temperature on Texture Change Rates

Texture change in foods may be due to chemical reactions occurring in the food; i.e. nonenzymatic browning, oxidative rancidity, or starch retrogradation. The reaction rates of these mechanisms have all been shown to be dependent on temperature. It is logical to assume that texture change is temperature dependent as well. The Arrhenius equation is widely used to describe the relationship of chemical reaction rates with temperature:

$$k = k_o \exp(-E/R\ T_a) \tag{3.5}$$

where:

k = rate constant, 1/s

k_o = Arrhenius constant, 1/s

E = Activation energy, kJ/mol

R = gas constant, 8.31441 J/mol K

T_a = Absolute temperature, K

3.4.2 Influence of Water Activity on Texture Change Rates

Rates of nonenzymatic browning and oxidative rancidity have been shown to be influenced by water activity. Quast and Karel (1972) developed a mathematical relationship between water activity and the rate constant for the deterioration of potato chips undergoing lipid oxidation. This relationship was a polynomial equation however, which contains several parameters that are difficult to obtain. A linear relationship between water activity and rate of browning was found by Martinez and Labuza (1968) in freeze-dried salmon. Water activity may also affect the rate of texture change as well. It would be useful to find a simple mathematical relationship to describe the role that water activity plays in texture change.

3.5 Influence of Packaging Film on Moisture Gain

The driving force for gases and vapors diffusing through permeable materials is the concentration gradient between the two surfaces of the packaging film. The rate of moisture transfer through a permeable membrane can be described by Fick's first law of diffusion:

$$f = -D \frac{dc}{dx} \tag{3.6}$$

where:

f = flux (the rate of moisture transfer per unit area of material), kg/(m^{2}s)

D = Diffusion coefficient of material, kg/(m s)

c = Concentration of diffusing substance, i.e. water

x = distance of permeation, m

If the diffusion coefficient (D) is independent of concentration (Perry,1973), Fick's law can be integrated to give:

$$f = \frac{D}{\ell} (c_1 - c_2) \tag{3.7}$$

where:

ℓ = film thickness, m

c = concentration of water (subscripts 1 and 2 refer to the outside and inside surfaces of the membrane respectively).

Henry's law,

$$c = Sp \tag{3.8}$$

is generally assumed to apply for polymers (Perry,1973), where:

c = concentration of moisture

S = solubility coefficient ,1/Pa

p = vapor pressure, Pa

For gas or vapor permeation, Henry's law can be combined with the integrated form of Fick's law, above, to give:

$$f = \frac{D}{\ell} (S_1 p - S_2 p) \tag{3.9}$$

Since the solubility coefficient is assumed a function of temperature only (Barrer,1941), and both membrane surfaces are at the same temperature then $S_1 = S_2 = S$ and:

$$f = \frac{P}{\ell} (p_1 - p_2) \tag{3.10}$$

where:

$$P = D\ S = \text{permeability constant} \tag{3.11}$$

A further substitution can be made with water activity, a_w, defined as the the vapor pressure, p, divided by the saturation vapor pressure, p_s, to give:

$$f = \frac{P}{\ell} p_s (a_{w,1} - a_{w,2}) \tag{3.12}$$

3.6 The Computer Simulation

There are only a few computer simulation models that are able to predict the rate of quality deterioration as a function of water activity by taking the effect of moisture penetration through the packaging film into account. Among these models, Quast and Karel (1972) first developed a

computer simulation to predict the storage life of potato chips undergoing deterioration by two mechanisms, loss of crispness and lipid oxidation.

Another computer model was presented by Purwadaria et al. (1979) utilizing a basic computer simulation proposed by Heldman (1974). Purwadaria et al. (1979) presented the iterative mathematical model to predict stability of ascorbic acid in a dry model food system.

Comparing computer simulations by Quast and Karel (1972) and Purwadaria (1977), the Purwadaria model is simpler and contains less parameters. A model similar to the Purwadaria model was developed for this study.

The model flow chart used for this study is illustrated in Figure 3.1. Whereas Purwadaria's model predicted ascorbic acid degradation, the model used in this study predicts texture of a pastry. Purwadaria's model incorporated the use of the Brunauer, Emmett, and Teller (1938) equation to predict water activity of the system as a function of moisture content whereas this model uses the Smith (1947) equation since it is suitable over a wider water activity range. This model will include an additional equation that considers the direct softening influence that water activity has on texture.

In the initial prediction steps, the computer model uses as input: 1) physical characteristics of the sample (initial moisture, m_o; initial texture, T_o; and product weight, w_p); 2) physical characteristics of the package

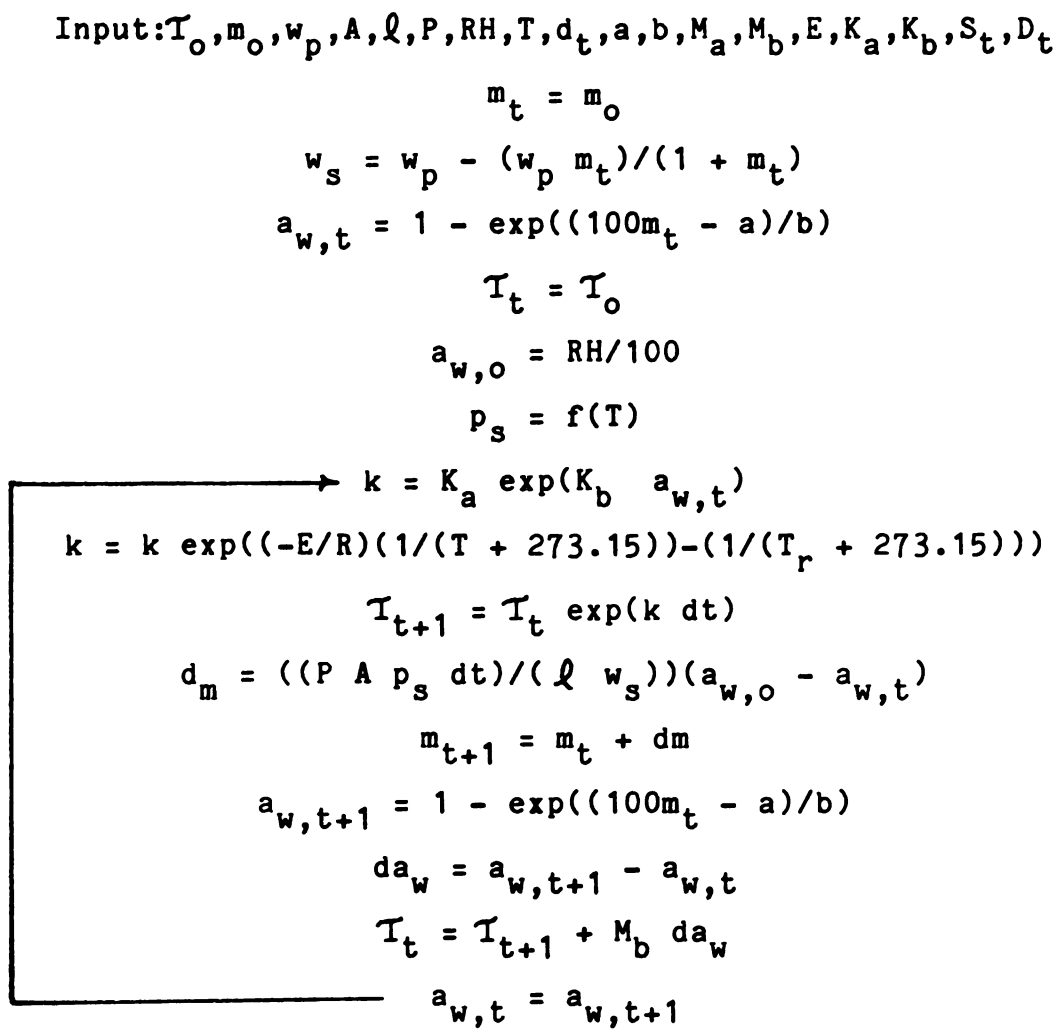

Figure 3.1 Model flowchart for prediction of moisture content and texture

(area, A; thickness, ℓ; and permeability constant, P); 3) the conditions of the storage environment (relative humidity, RH; and temperature, T); and 4) the time variables (iterative time increment, dt; storage time, S_t; and display increment, Dt). Constants for the Smith isotherm equation (a and b), linear regression constants that describe the direct effect of moisture on texture (M_a and M_b) and constants describing the effect of temperature (activation energy, E) and constants describing kinetic rate constants as a function of water activity (K_a and K_b) may be used either as inputs or incorporated into the computer program. The program calculates the outside water activity, solids weight of the product, saturation vapor pressure (Madsen,1981), and initial product water activity before entering the loop. The rate constant , k, for texture change is first calculated as a function of water activity and temperature. The texture , τ, at time, t, is then calculated from the rate constant. Over the time period, dt, the amount of moisture that permeates through the package material, dm, is calculated. This moisture is taken up by the product and new moisture content, m_{t+1}, determined. From the new moisture content, the new water activity, $a_{w,t+1}$, is calculated from the Smith isotherm equation. The change in water activity over the time period, dt, is then calculated. This allows for the new texture, τ_t to be calculated as a direct result of moisture increase or decrease. This completes the loop and calculations are

directed back to the point where rate constants are determined again as a function of water activity. Outputs of time, water activity, moisture content, texture, and rate constant are displayed at predetermined intervals. Iterative calculations stop when the total storage time is reached.

IV. EXPERIMENTAL

4.1 Model System and Preparation

A baked pastry was used throughout this investigation. The formulation of the model system is a modification of a Spritz cookie recipe obtained from Better Homes and Gardens New Cook Book (1981). The ingredients are common to a variety of cookies, breakfast bars, and other pastry-like items.

The composition of the model system was as illustrated in Table 4.1. The flour and baking powder were stirred together by hand in large stainless steel bowls. The margarine was beat separately for 30 seconds in a Duoflex mixer (Artoflex Corp.). Sugar was added to the margarine until the mixture was fluffy. Beaten eggs and vanilla were also added and beat until smooth. The dry ingredients were gradually added to the beaten mixture until well blended. The mixture was divided into 5 kg. portions and pressed into 0.007 m slabs with an Anets Production Table (Anets Berger Corp.). The slabs were cut into approximately 0.2 m lengths and laid onto cookie pans lined with wax paper. The pans were placed in Rotorack ovens (Cox-Denholm) and baked at 204 C for a period of 9 minutes. After removal from the oven,

Table 4.1 - Composition of model food system

Component	% by weight
All-purpose flour	42.78
Margarine	35.71
Sugar	16.16
Eggs	4.39
Vanilla	0.52
Baking powder	0.44

the pans were allowed to cool for five minutes. Circular cookie cutters (0.051 m diameter) were pressed into the slabs to make the pastries, resulting in a baked pastry with uniform thickness and diameter. The pastries were then laid between layers of waxed paper 3 deep. The boxes were placed in -2 C frozen storage at least 24 hours before equilibration or packaging and storage.

4.2 Moisture Equilibration

After preparation, the pastries were equilibrated to temperatures and relative humidities by two different methods; dynamic equilibration, and static equilibration.

4.2.1 Dynamic Equilibration Method

The dynamic equilibration system is illustrated in the schematic diagram in Figure 4.1. The pastries were placed in an insulated equilibration chamber maintained at constant relative humidity and temperature using an air conditioning unit (Aminco Aire Cat. No. 4-5460).

The desired temperature and relative humidity were established by controlling the temperature of a water bath and the dry bulb temperature of air circulated over the bath. The fan in the Aminco Aire drew air from the test chamber through a spray of fine water droplets drawn from the water bath. Heat and water vapor were exchanged between the water droplets and the stream of equilibration chamber

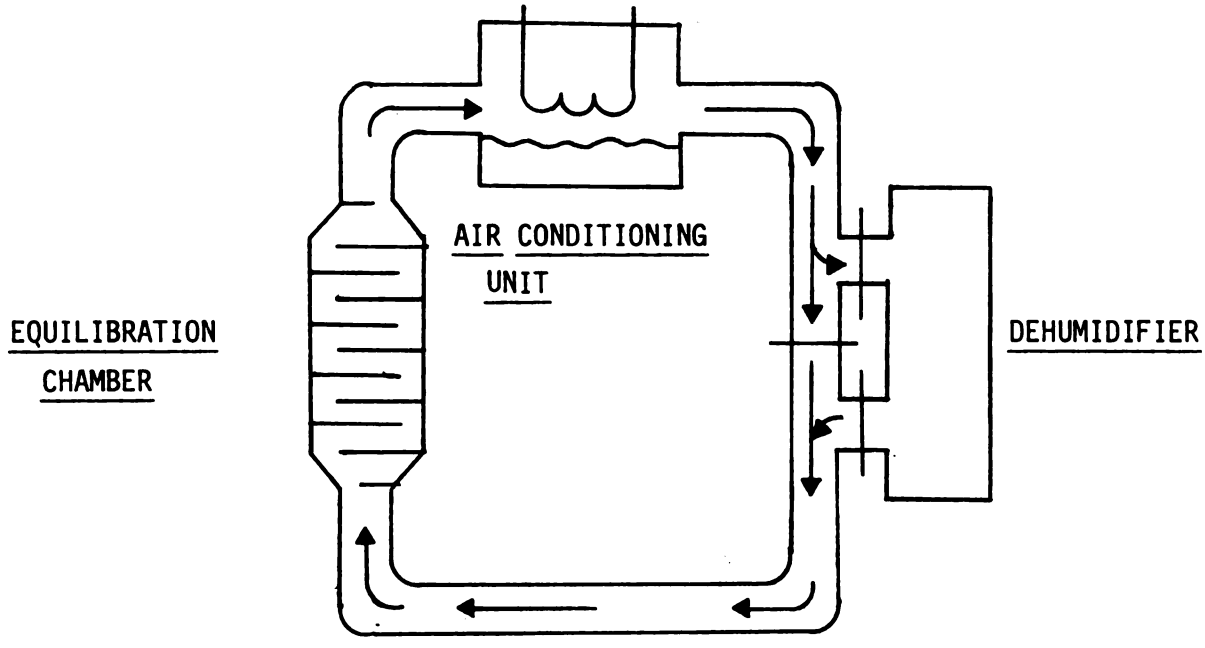

Figure 4.1 Schematic diagram of equilibration system

air until equilibration was reached, and the dew point of the air was fixed. The air was then heated to the desired dry-bulb temperature by electric heaters controlled by a thermoregulator and was returned to the equilibration chamber. As this process was continuous, properly conditioned air was circulated through the equilibration chamber, assuring uniformity of humidity and temperature. The equilibration chamber was constructed of plywood and heavily insulated with polyurethane foam. Rubber seals were placed near the door to prevent air leakage and thereby maintaining a closed system. Soft foam was placed on the back of the chamber door to conform to the chamber shelving. The shelves were designed with slots placed in the sides in an alternating pattern (See Figure 4.1). This forced air to pass over the product while traveling on to the next shelf. For low humidity conditions, the Aminco-Aire unit did not generate sufficient dry air. In these instances, a Cargo-Aire Dehumidifier was placed in the air conditioning system loop to remove water from the air. Since the dehumidifier generated excessive heat, the dehumidified air was passed through a heat exchanger to cool the air before returning to the Aminco Aire unit.

In order to measure temperature and relative humidity inside the chamber copper-constantan thermocouples were placed in the airstream. One thermocouple was left bare and the other was covered with a wetted sock to measure dry and wet bulb temperatures respectively. The thermocouples were

connected to a Hewlett Packard 3497 Data Acquisition system and Hewlett Packard 85A microcomputer. Relative humidities were calculated from the wet bulb and dry bulb temperatures (Madsen,1981). Equilibration times ranged from four to seven days for adsorption and desorption.

4.2.2 Static Equilibration Method

Very low relative humidity conditions (30% at 10 C) were not achievable using the dynamic equilibration apparatus. For these conditions, pastries were equilibrated in a closed container containing a saturated MgCl solution maintained at a relative humidity of 33.8% RH at a controlled constant temperature of 10 C. Pastries were removed after approximately 14 days, when no weight change was observed between three successive weighings. Weighings were taken approximately 12 hours apart after the first 4 days of equilibration.

4.3 Moisture Content Determinations

The moisture contents of the pastries were determined by a modified vacuum oven method described by AOAC Method 14.003 (1980). Pastries were placed in aluminum weighing dishes and weighed. The pastries were dried at 98-100 C for about 5 hours in a vacuum oven with a pressure of 3.33 kPa or less. After cooling in an air-tight desiccator with

activated drying agent, the sample was weighed and moisture content was calculated.

The moisture contents of the pastries during equilibration and storage were obtained by measuring the weight change of the sample compared to the initial weight of the sample. By knowing the moisture content in the initial sample (using AOAC method 14.003 (1980)), the moisture content during storage and equilibration was calculated. The weight change of the sample was measured by using a Mettler P1920 Analytical Balance.

4.4 Measurement of Sorption Isotherms

Pastries were placed in aluminum weighing dishes, weighed, and equilibrated to a range of relative humidities and temperatures by one of the two equilibration methods. See Table 4.2 for the ranges of relative humidities and temperatures used. After samples reached constant weight final weights were used to obtain moisture contents on a dry weight basis (g H_2O/100 g solids).

At each temperature, a sorption isotherm was obtained by plotting the dry basis equilibrium moisture content versus equilibrium relative humidity (E.R.H.) or water activity (a_w) (E.R.H./100 = a_w). Least squares regression analysis of the isotherm data was conducted to obtain the Smith constants, a and b, for the desorption portion of the isotherm.

Table 4.2 - Experimental equilibrium temperatures and water activities

	Temperature, C			
	10	20	32	43
		0.18	0.21	
Equilibrium	0.33	0.30	0.30	0.30
Water		0.44	0.45	
Activity	0.60	0.60	0.60	0.60
		0.73	0.74	

4.5 Measurement of Texture

Two measurements generating three different texture parameters were used to characterize the texture of the pastries. All three mechanical measurements of texture involved the use of an Instron Universal Testing Apparatus, floor model TTBM, set at high sensitivity and equipped with a 1 - 50 kg load cell. A crosshead speed of 1 cm/min was used for all measurements.

4.5.1 Texture Profile Analysis

A 0.0095 m diameter probe was chosen for the Texture Profile Analysis. Pastry thickness was measured with calipers before placement under the probe and on the load cell. Force was applied on the pastry to a deformation of 10% of pastry thickness in two cycles. A typical response of the sample to the applied force is illustrated in Figure 4.2. Two of the Texture Profile Analysis parameters were measured. The procedures used in computations were similar to those described by Bourne (1968), and were defined as follows:

Hardness, H (Newtons) = magnitude of H

Cohesiveness, $C = A_2/A_1$

This technique was used to determine Hardness and Cohesiveness at five different locations on each pastry; once in the center and at four equally spaced positions

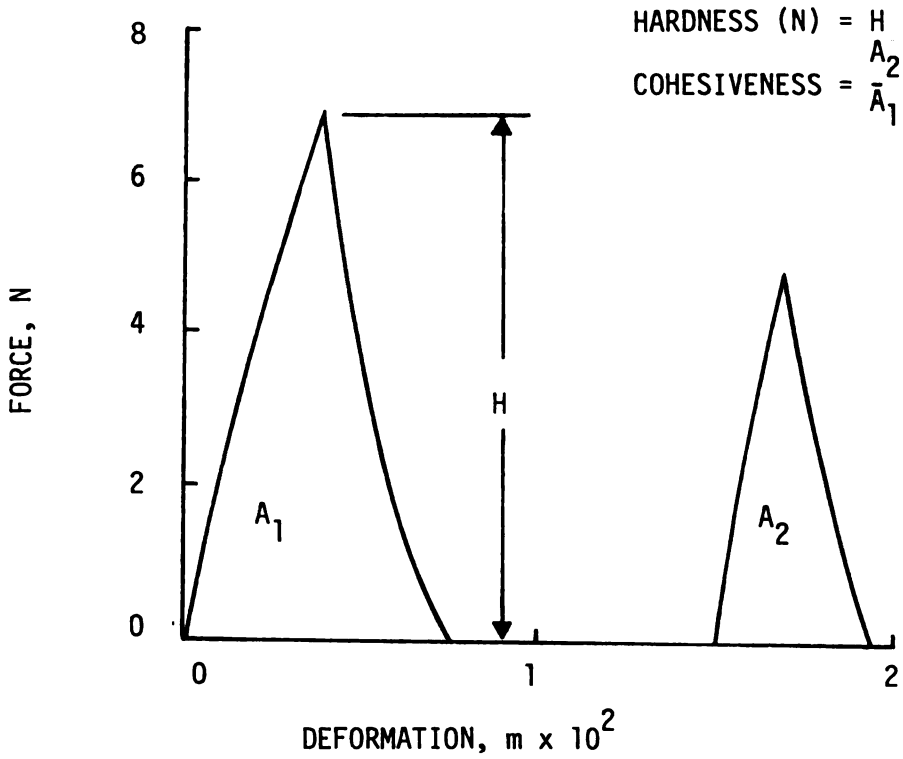

Figure 4.2 Typical force-deformation curve for texture profile analysis

surrounding the center and 0.00635 m from the edge. See Figure 4.3.

4.5.2 Bending Test

Each pastry was suspended over 0.03 m wide bridge and force was applied with a 0.0095 m diameter bar to the pastry. See Figure 4.4. A typical response of the sample to the applied force is illustrated in Figure 4.5. The force (F) required to fracture the pastry was divided by the pastry thickness (L) to obtain a breaking force per unit depth of pastry, B, or:

$$\text{Bending Value, B (N/m)} = F/L$$

4.6 Measurement of Texture Change Rate as a Function of Water Activity and Temperature

The pastry model system was prepared (section 4.1) and equilibrated (section 4.2) to the conditions represented in Table 4.2. Two equilibrated pastries were then placed in each of 0.175 m x 0.125 m impermeable foil pouches and immediately sealed. The pouches containing the equilibrated samples with water activities near 0.20, 0.45, and 0.75 were stored in a room with a controlled temperature of 20 and 32 C. The pouches had zero permeability so moisture contents and water activities were assumed to hold constant over the entire storage period. The pouches containing the

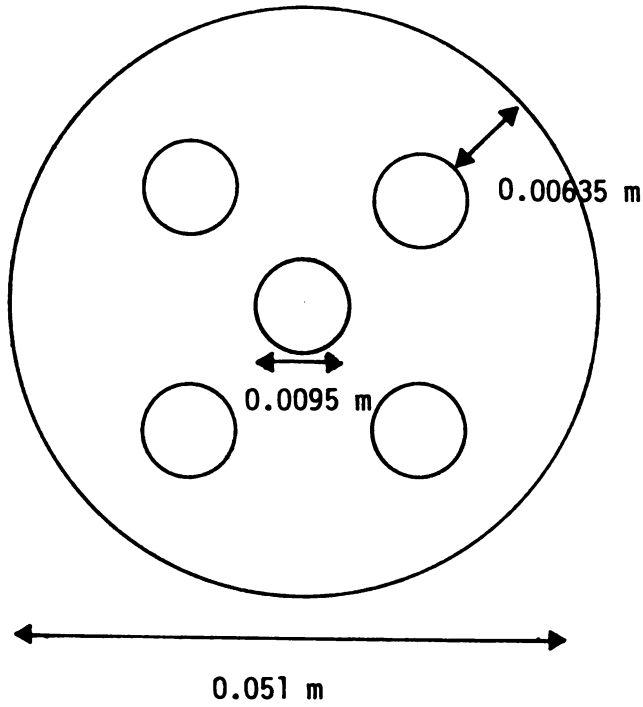

Figure 4.3 Pastry locations for measuring texture profile analysis

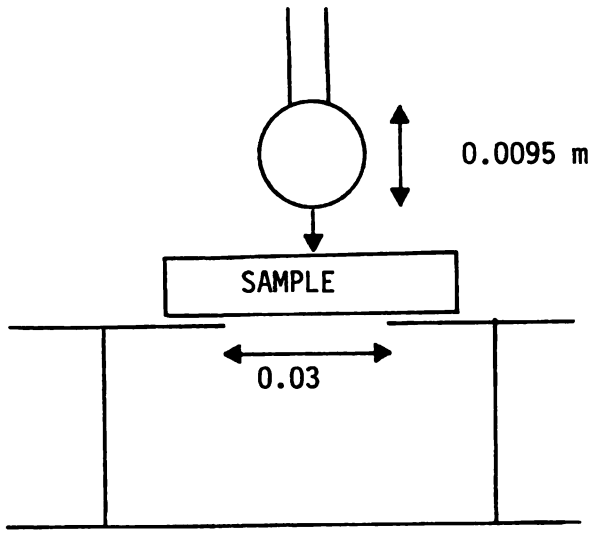

Figure 4.4 Apparatus for measuring bending value

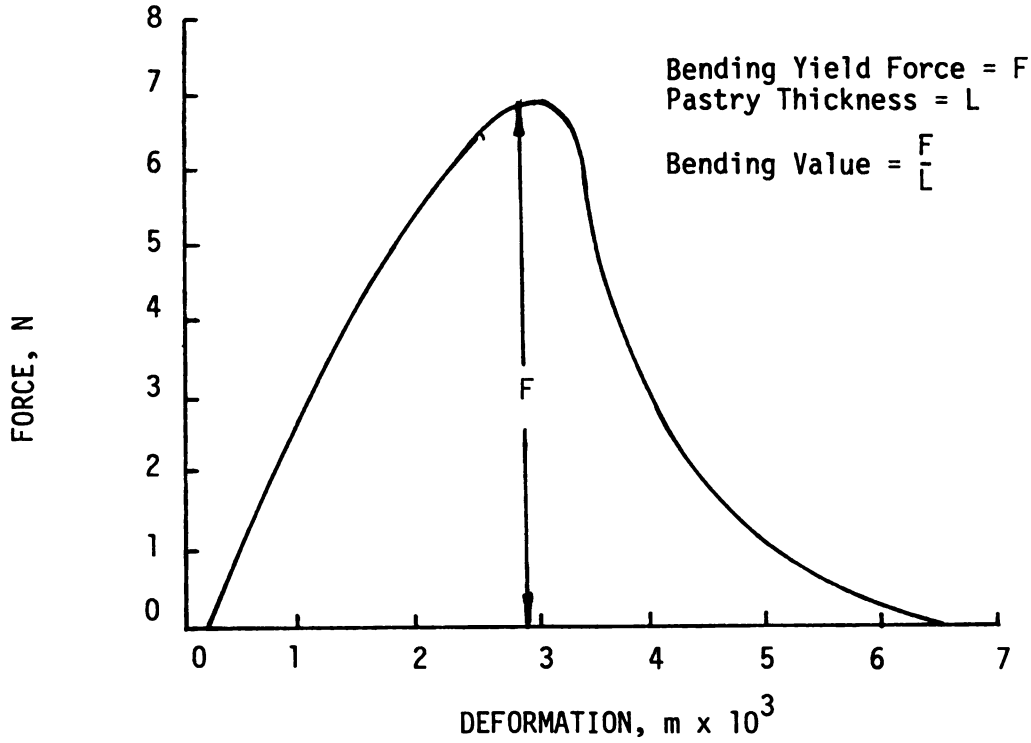

Figure 4.5 Typical force-deformation curve for bending value

equilibrated sample with water activities near 0.30 and 0.60 were stored in rooms with controlled temperatures of 10, 20, 32, and 43 C.

Three pouches were sampled from each room at each time period, water activity, and temperature and brought to 21 C before measuring texture. Texture Profile Analysis (Section 4.5.1) was performed on one pastry from each pouch in the group. Bending tests were performed on the remaining pastries from a given pouch.

The rate constant for texture change was obtained by plotting texture versus time at each condition. The relationship between the rate constant and temperature was obtained by plotting the rate constant versus inverse absolute temperature with the water activity of storage held constant. The relationship between the rate constant and water activity was obtained by plotting the rate constant versus water activity with the temperature of storage held constant.

4.7 Model Verification Experiments

Three packaging films were chosen for the model verification experiments to manufacture pouches with the following dimensions: Polystyrene film with 5.46×10^{-5} m thickness, 0.110 m width, and 0.190 m length; Polyethylene film with 5.08×10^{-5} m thickness, 0.95 m width, and 0.175 m length and; Foil pouch material with 7.62×10^{-5} m thickness, 0.125 m width, and 0.175 m length. Two pastries

with moisture contents of 11.82% were placed in each package and sealed immediately to minimize moisture migration between the model and the atmosphere. The packages containing the pastries were stored in rooms at different temperatures (10, 20, 32, and 43 C) at 30 % RH, and at different relative humidities (30, 45, 75, and 90% RH) at 20 C.

Three packages were removed from each room at various time intervals over a 4 month period. Total weight and moisture content were recorded and texture measurements were conducted and recorded.

4.8 Measurement of the Permeability Constant for Packaging Films

The rate of water vapor transmission through the packaging film was determined by the standard method for water vapor transmission of materials in sheet form (ASTM E-96-66). Fifteen grams of activated anhydrous calcium sulfate were sealed in a standard aluminum test cup by the test film and wax. The cup is placed in a chamber maintained at a constant temperature and relative humidity. The gain in weight is determined and plotted as a function of time. Permeability constants were calculated at 10, 21, 32, and 43 C at 30% RH (the conditions maintained in the controlled atmosphere rooms) to determine influence of temperature on moisture transfer.

V. RESULTS AND DISCUSSION

5.1 Measurement of Permeability Constants

The permeability constants (P) for the packaging films were measured at a constant relative humidity of 30% at temperatures of 10, 20, 32, and 43 C. The permeability constants for the three packaging films used are in Table 5.1. These results indicate that temperature does not have a significant influence on the permeability constant for polystyrene ($P = 6.27 \times 10^{-15} \pm 0.03 \times 10^{-15}$ kg m/m^{2}s Pa). This is in close agreement with the value obtained by Doty et al. (1946) of 6.25×10^{-15}kg m/m^{2}s Pa. However, permeability constants for polyethylene are affected by temperature in a significant manner. The results in Figure 5.1 indicate that the temperature dependency of the permeability constant (P) for polyethylene can be described by the Arrhenius relationship:

$$P = P_o \exp(-E/R\ T_a)$$

where:

$P_o = 3.43 \times 10^{-9}$ kg m/m^2 s Pa

= Arrhenius constant for permeability constant

E = 37.2 kJ/mol

R = 8.31441 J/mol K

Table 5.1 - Permeability constants (P) for polystyrene, polyethylene, and foil pouch material at 10, 20, 32, and 43 C and 0.30 water activity

	$P \times 10^{15}$ $((kg\ H_2O\ m)/(m^2\ s\ Pa))$		
Temperature, C	Polystyrene	Polyethylene	Foil Pouch
10	6.26	0.48	0.00
20	6.30	0.82	0.00
32	6.30	1.48	0.00
43	6.24	2.50	0.00

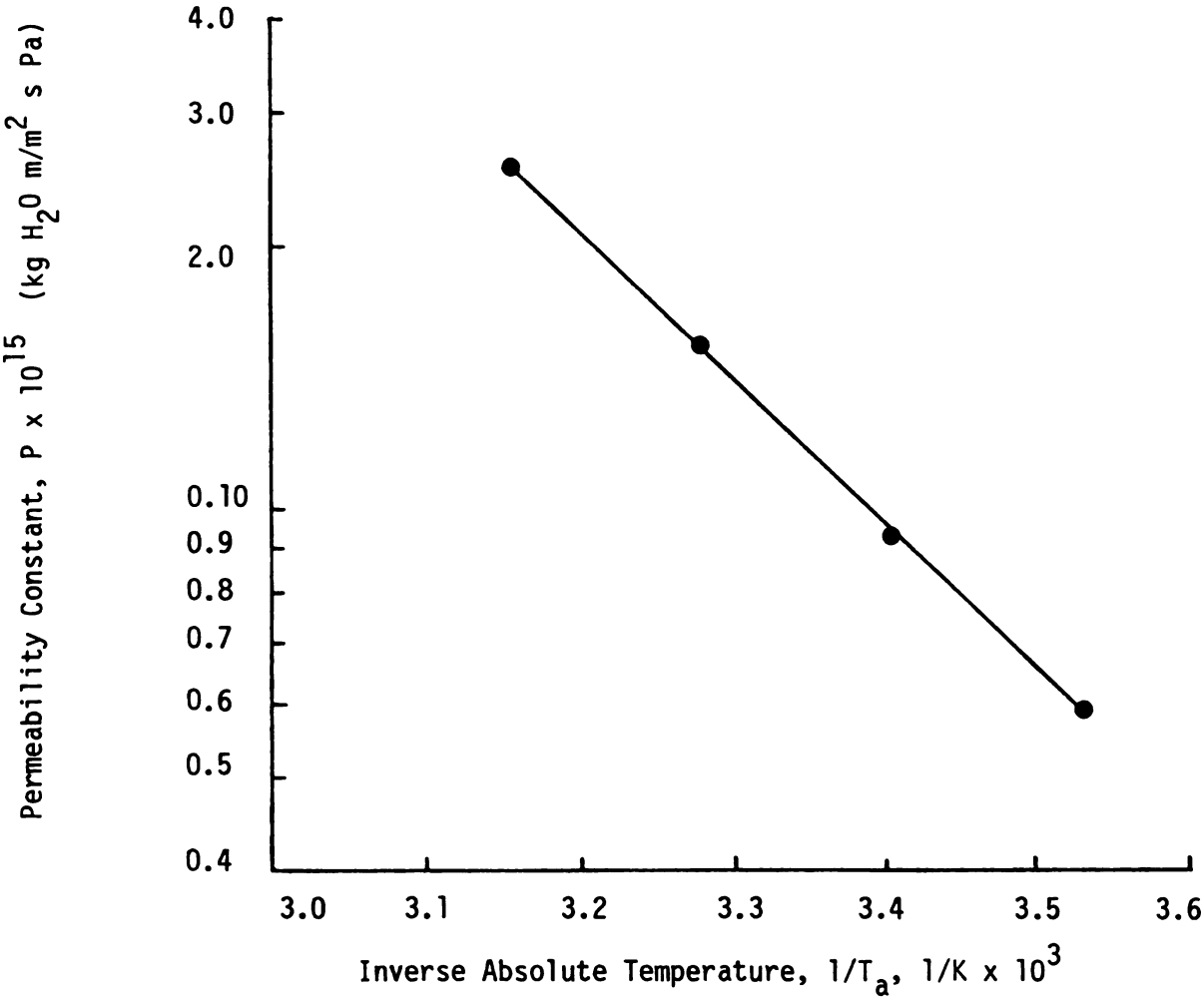

Figure 5.1 Arrhenius plot of permeability constant for polyethylene film

These values are similar to those of Doty et al. (1946) where E was found to be 43.2 kJ/mol and P_o was 1.43 x 10^{-8} kg m/m^2 s Pa.

5.2 Sorption Isotherms

The sorption isotherms obtained by measuring the equilibrium moisture content at various water activities and four different temperatures (10, 20, 32, and 43 C) are presented in Figure 5.2. Figure 5.2 contains adsorption and desorption points. The original product moisture content was 11.82 kg H_2O/100 kg solids. Pastries were equilibrated to the desired water activities from that reference point. So isotherm points above 11.82 kg H_2O/100 kg solids are exhibiting adsorption whereas points below the original product moisture exhibit desorption.

Desorption isotherm data measured in this study were analyzed using the Smith (1947b) equation as a model. The Smith parameters, a and b, were evaluated using least squares analysis. See Table A.1 for isotherm data. The desorption data at 20.1 C was described by a regression line between water activities of 0.18 and 0.60 with Smith constants ,a and b, of 2.46 and -7.47 respectively. No regressions were generated for adsorption because only one adsorption point was generated above the original 11.82 % moisture content.

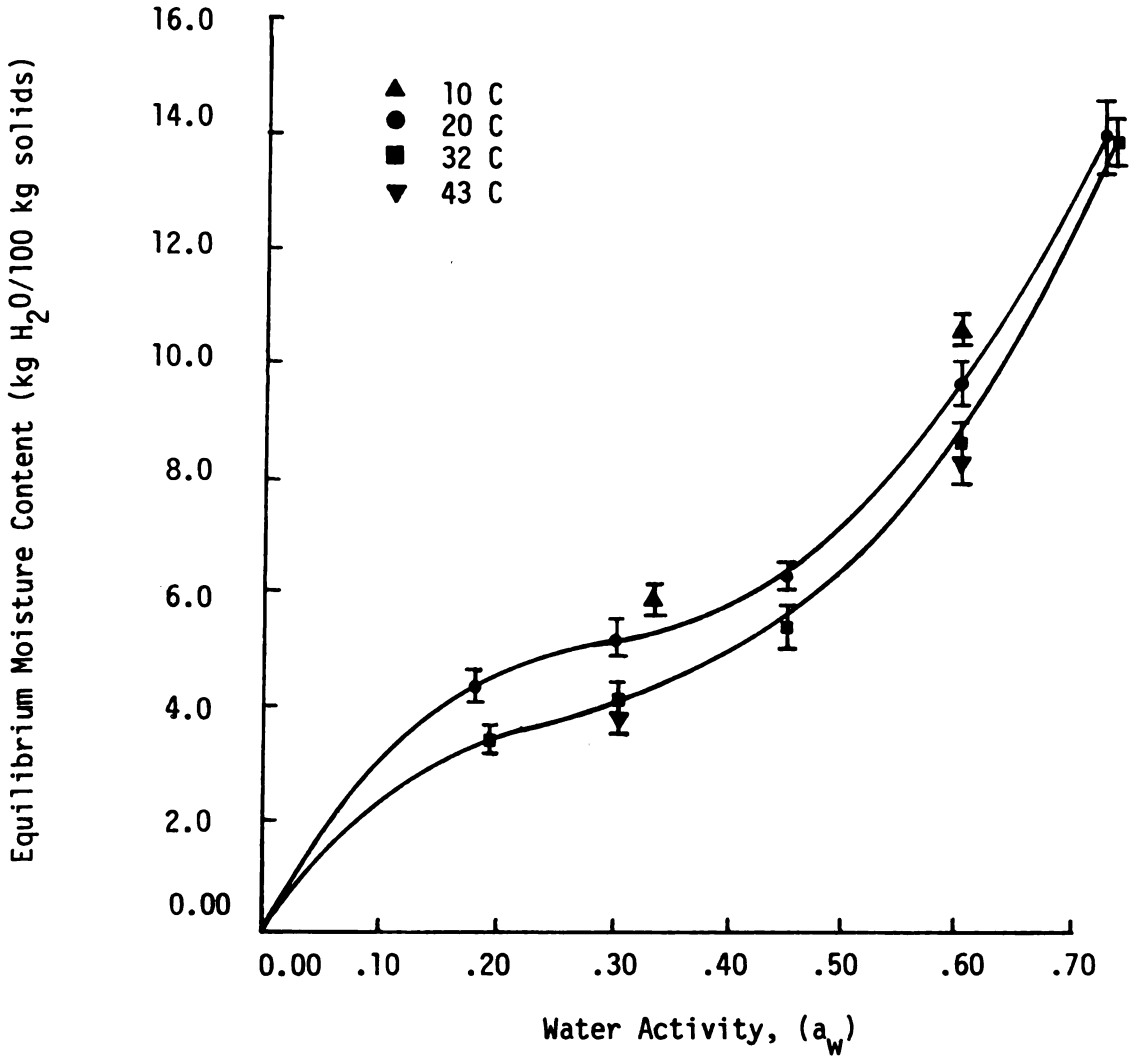

Figure 5.2 Moisture isotherms at 10, 20, 32, and 43 C

5.3 Effect of Water Activity and Temperature on Initial Texture

The relationship between initial hardness (H_o) and water activity indicates a linear relationship at water activities above 0.2 as illustrated in Figure 5.3. The curves were drawn from data available in Table A.2. Increasing water activities above 0.2 result in decreasing initial hardness values. Higher equilibration temperatures seem to elevate initial hardness values when water activity is held constant. This may be due to hardening during the equilibration period which occurs faster at higher temperatures. The lower hardness values below water activity of 0.2 may be a reflection on the importance of water in structural strength above monolayer moisture levels. At water activities below 0.2, pastries may not have enough water to develop a network of hydrogen bonding to increase the structural strength of the pastry.

Similar curves for initial measurements of cohesiveness (C_o) and bending value (B_o) are illustrated in Figures 5.4 and 5.5 respectively. The curves were drawn from data available in Tables A.3 and A.4. It can be seen that initial cohesiveness measurements increase with increasing water activity and minimum values are observed around water activities of 0.3. Increasing cohesiveness values at higher water activities reflect the viscoelasticity or springiness of a pastry at higher moistures. There is a corresponding loss of springiness and decrease in viscoelasticity with

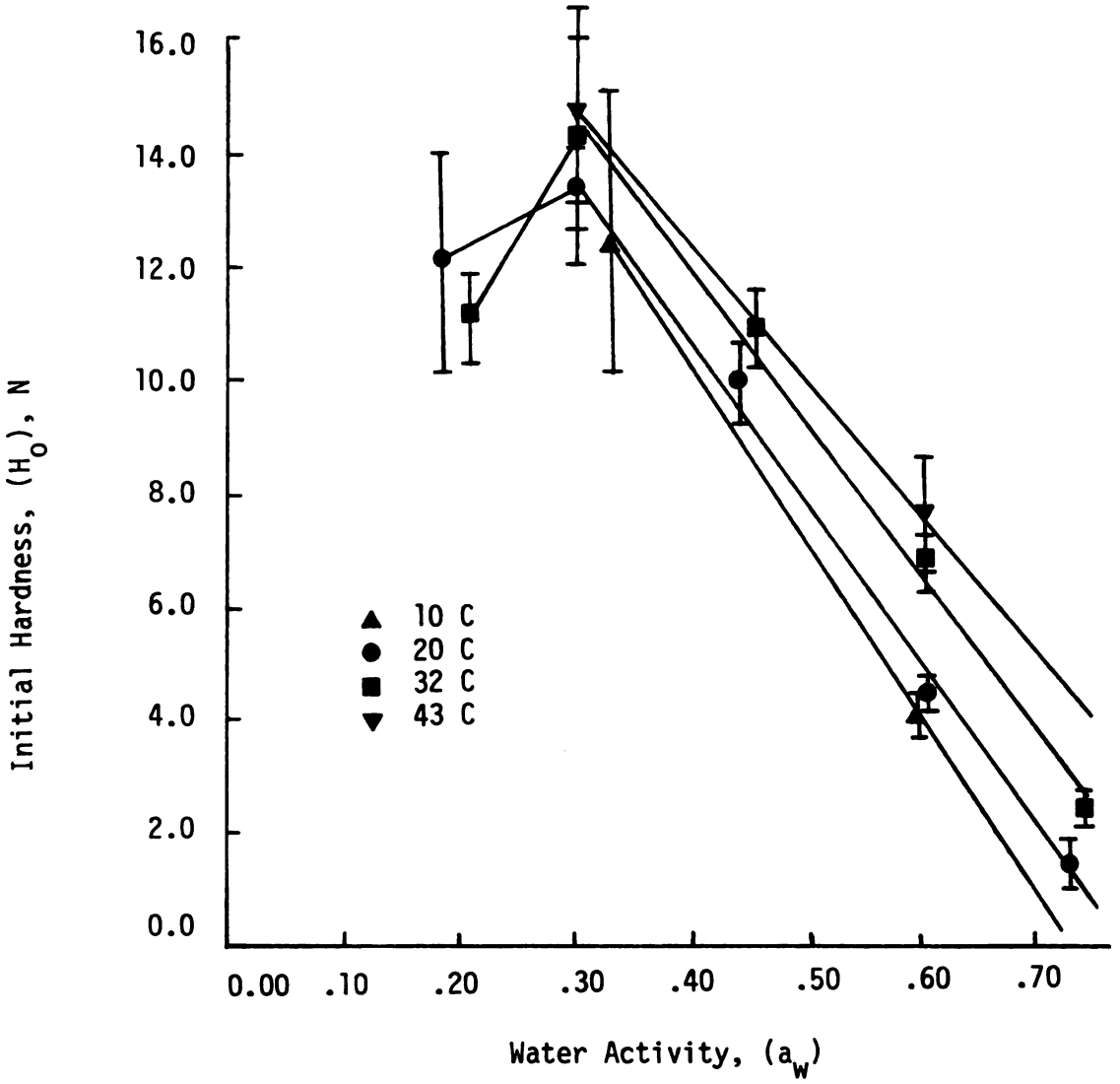

Figure 5.3 Initial hardness vs. water activity at 10, 20, 32, and 43 C

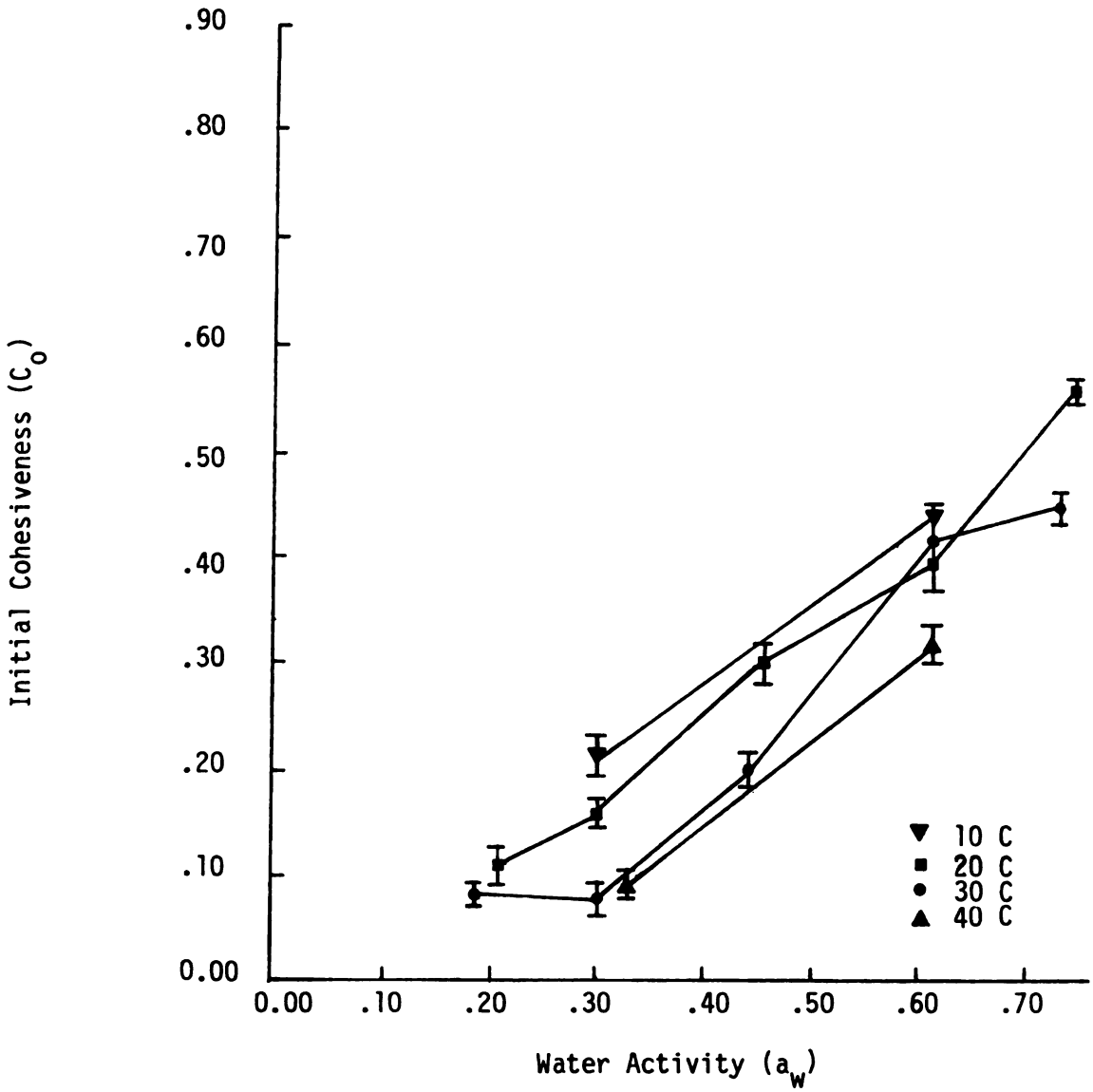

Figure 5.4 Initial cohesiveness vs. water activity at 10, 20, 32, and 43 C

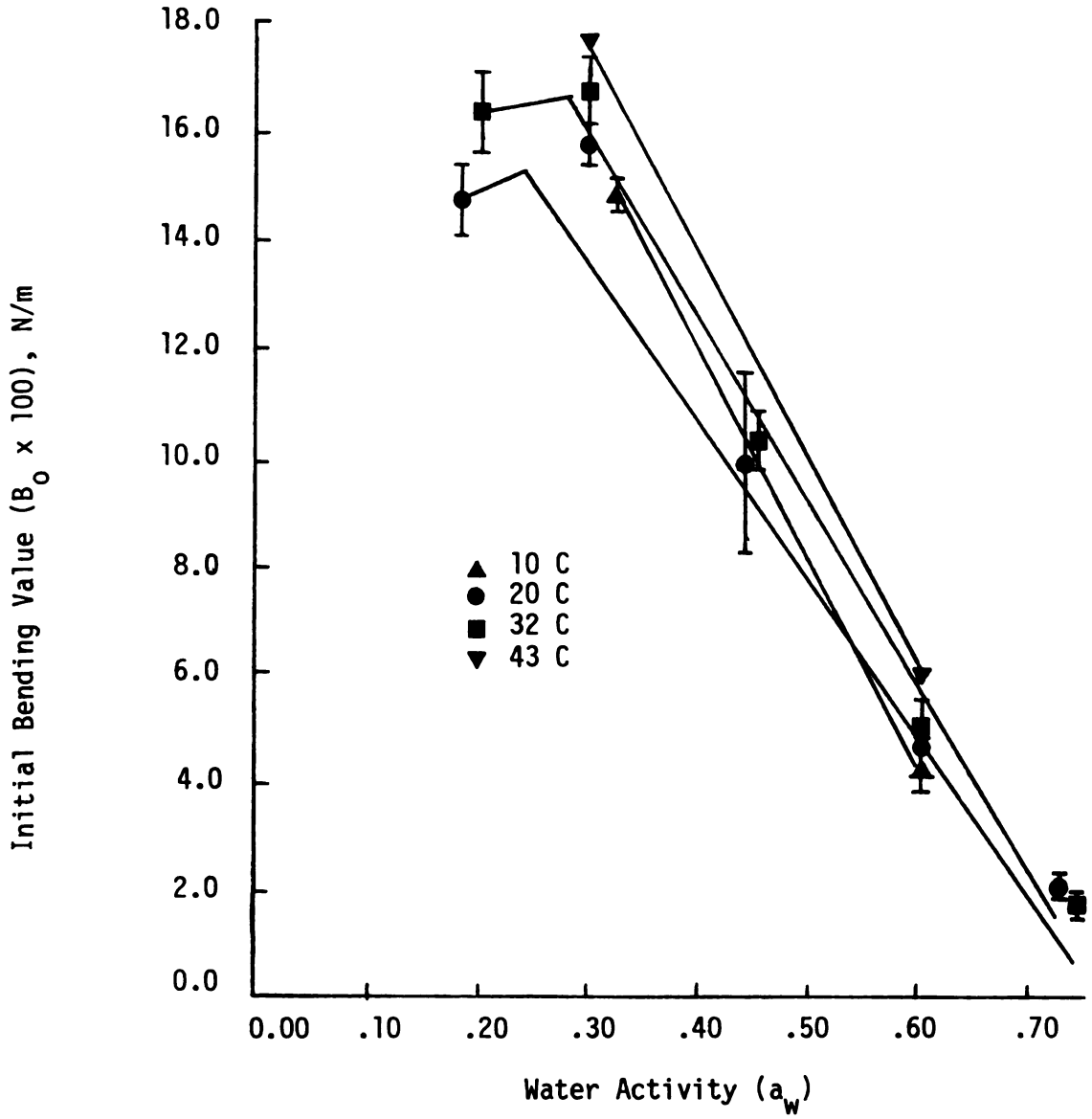

Figure 5.5 Initial bending value vs. water activity at 10, 20, 32, and 43 C

drier, low moisture pastries. Bending values, on the other hand decrease with increasing water activity and maximums occur around water activies of 0.3. The bending value and hardness measurements seem to be closely related to each other in their relationship to water activity. They both decrease with increasing water activity. Their magnitudes are very similar as well. More hardness measurements were taken than bending values however, providing for a larger statistical sampling and more reliable results.

5.4 The Order of Rate Constant

Kinetic analysis for the different constant environments using zero order and first order relationships indicates no significant difference between a zero and first order relationship based on the magnitude of the correlation coefficient, r^2. This is illustrated in Figure 5.6 where both the zero order and first order regression lines were plotted for samples stored at 20 C and a water activity of 0.60.

It was decided to use the first order relationship on the basis that the chemical and/or physical reactions that may be responsible for texture change have all been described by first order rate constants (See Section 2.3).

A peculiar phenomenon occurred in the pastries that was not accounted for in calculation of rate constants. Texture values tended to reach maximums after a certain length of time before decreasing. Rate constants were calculated

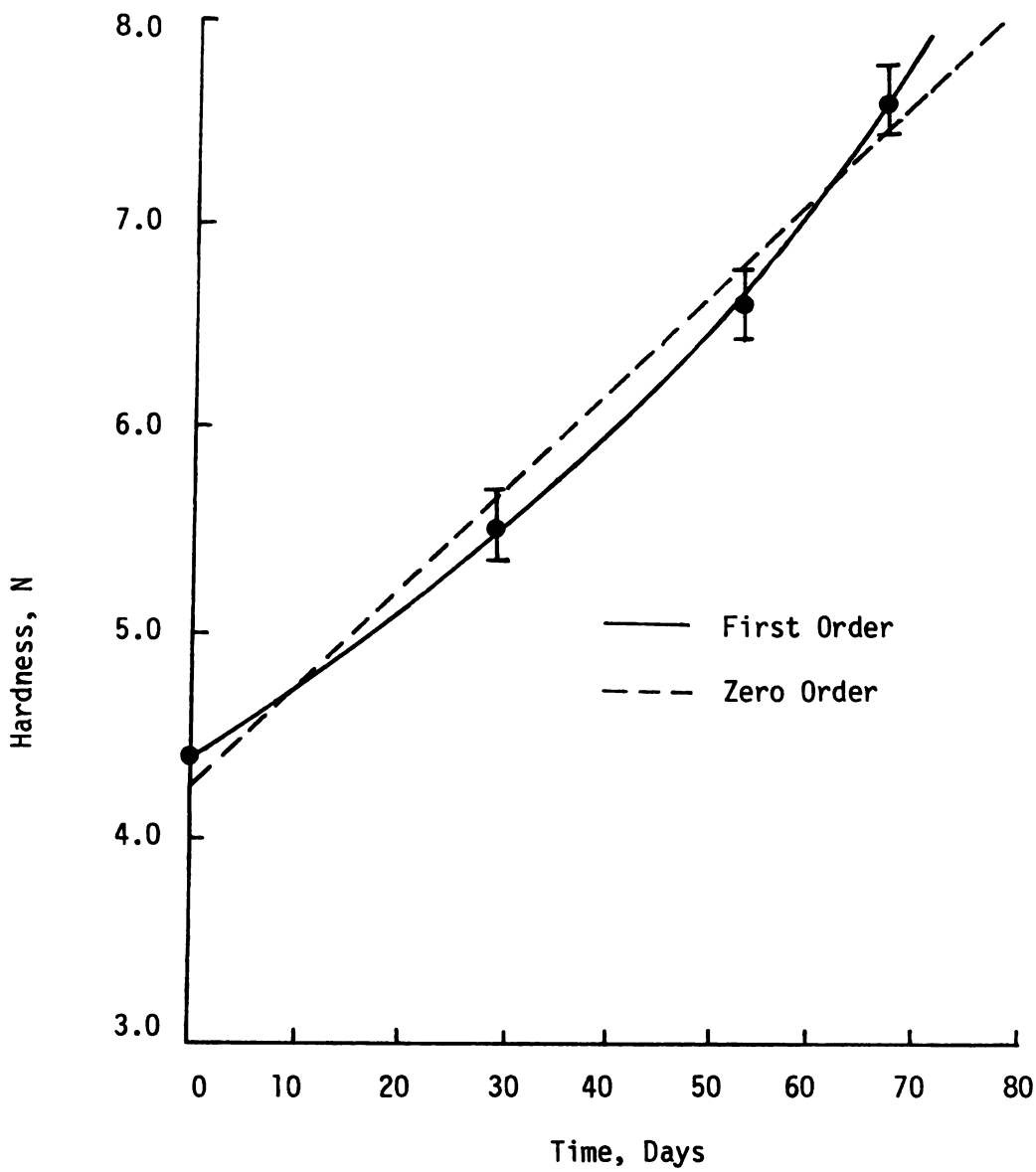

Figure 5.6 Zero and first order regression lines describing change in hardness for pastries stored at 20 C and 0.60 water activity

using points before texture values started to decrease. This phenomenon is discussed in more detail in Section 5.8.

5.5 Effect of Water Activity on Rate of Texture Change

The effect of water activity on the rate constant for change in hardness is illustrated in Figure 5.7 which were drawn from data available in Table A.8. These results suggest that the rate constants increase exponentially with water activity. The data were analyzed with a least-squares analysis on the rate constant values for change in hardness as a function of time. The following exponential relationships were obtained:

$$k = 1.02 \times 10^{-8} \exp(3.68\ a_w) \text{ at } 20C,\ r^2 = 0.98$$
$$k = 1.57 \times 10^{-8} \exp(4.30\ a_w) \text{ at } 32C,\ r^2 = 0.99$$

The influence of water activity on rate constants for changes in cohesiveness and bending value are presented in Figures 5.8 and 5.9 respectively (See Tables A.9 and A.10 for actual data). Rate constants for change in cohesiveness tend to remain constant or decrease to a minimum at a water activity of 0.60 and increase again rapidly at higher water activities. Because of these two transition points it was not possible to obtain a simple mathematical relationship to adequately describe the influence of water activity on cohesiveness. Nor could any one type of relationship be found to adequately describe water activity's influence on

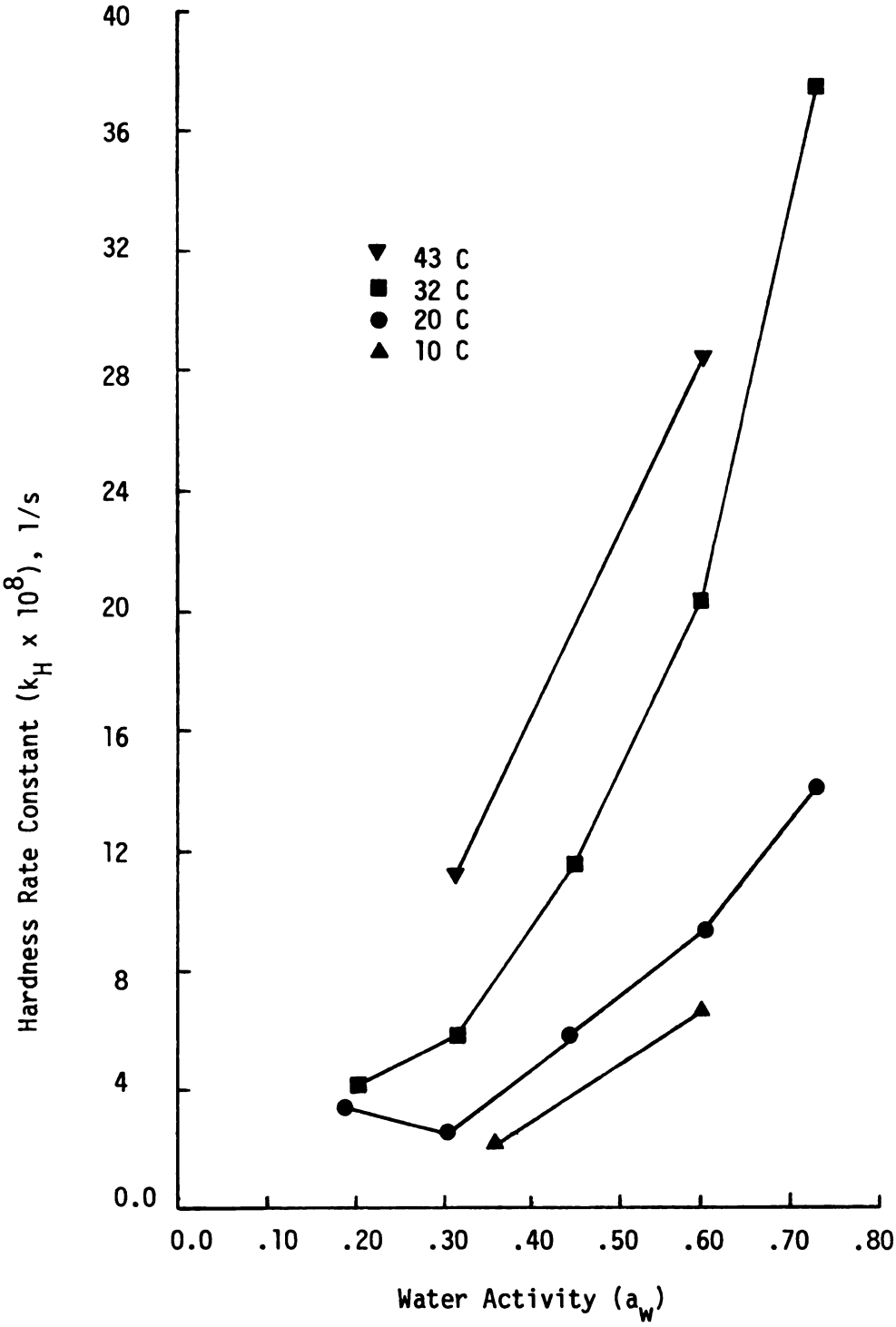

Figure 5.7 Rate constant for change in hardness vs. water activity at 10, 20, 32, and 43 C

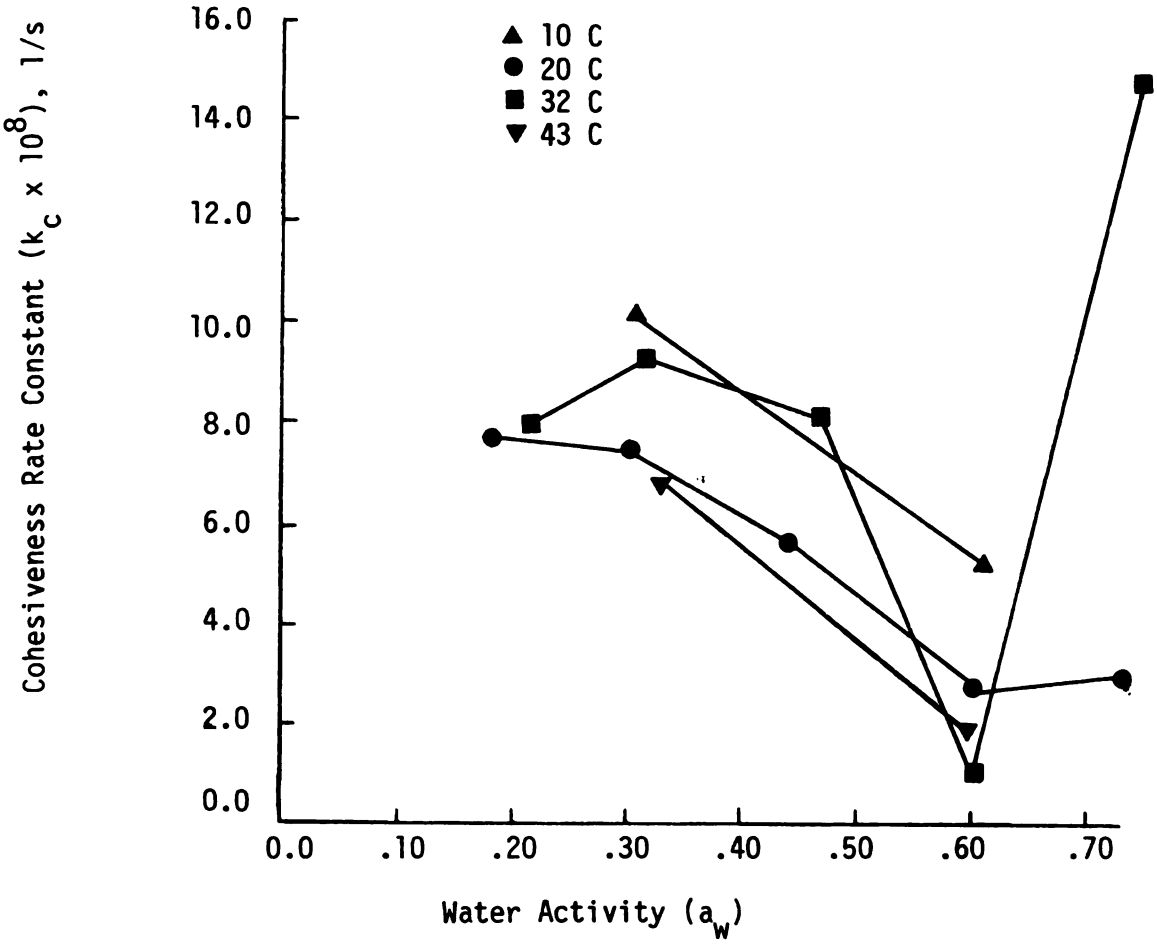

Figure 5.8 Rate constant for change in cohesiveness vs. water activity at 10, 20, 32, and 43 C

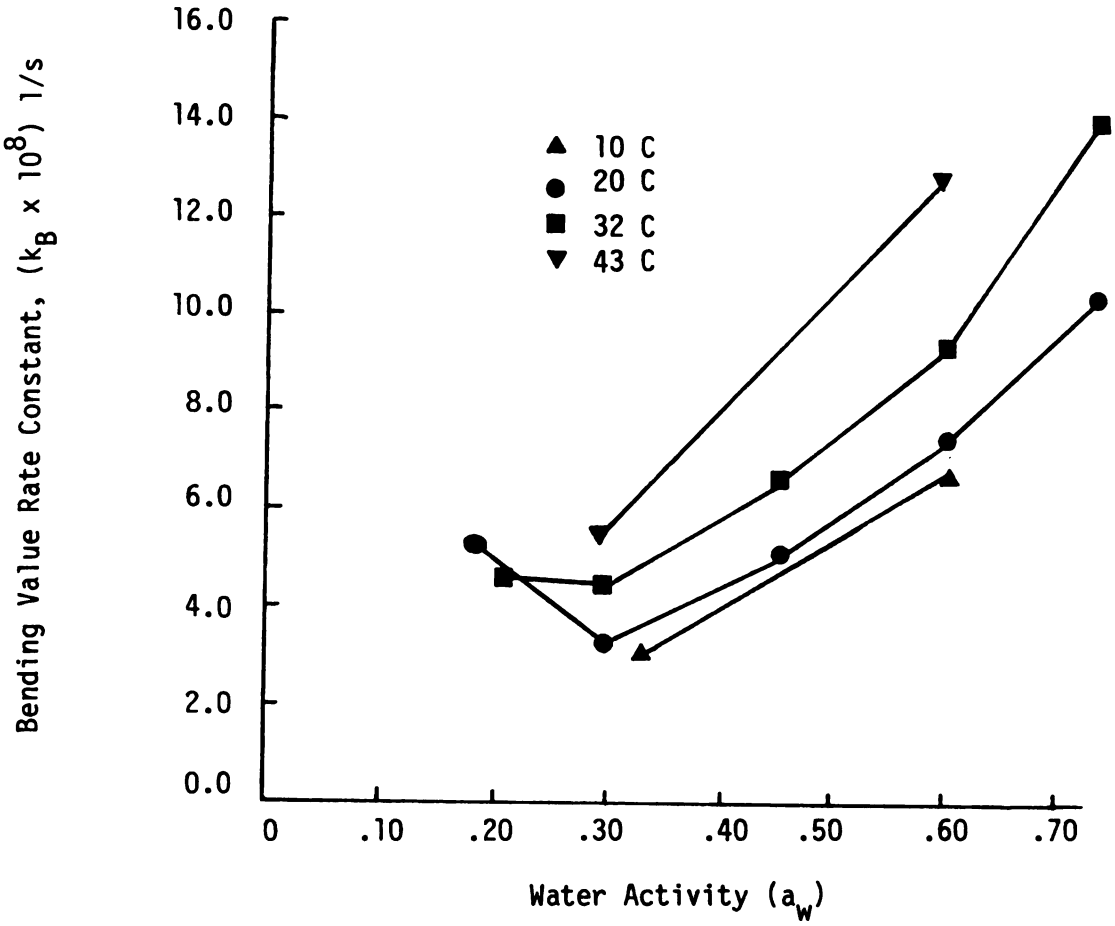

Figure 5.9 Rate constant for change in bending value vs. water activity at 10, 20, 32, and 43 C

cohesiveness over a range of temperatures. For these reasons, cohesiveness proved to be an impractical choice as a measurement for description of the textural properties of the pastry used in this study. It also prohibited it from being a measurement that would adequately demonstrate the capabilities of the computer model. The inconsistencies of the relationships between the rate constants for cohesiveness and water activity may have been due to the sensitivity of the cohesiveness measurement in relationship to the hardness measurement. A second cycle is required to obtain the cohesiveness value. If the pastry is cracked, the second cycle will not result in a response necessary for a proper cohesiveness measurement. This is not always detectable from observation but may affect the magnitude of the measurement. This may be further aggravated over time and at lower water activities where drier pastries crack more easily. Rate constants for change in bending value increase with increasing water activity and tended to follow relationships similar to the way rate constants for change in hardness behaved in relation to water activity. The sampling for measurement of bending value was not as large as the sampling for measurement for hardness however, and were not as reliable a measurement as hardness. For these reasons, hardness was selected from the three texture measurements as the texture measurement of choice for the computer model prediction of texture for the model pastry used in this study.

5.6 Effect of Temperature on Rate of Texture Change

The influence of temperature on the rate constants for change in hardness is illustrated in Figure 5.10 using an Arrhenius relationship where $k = k_o \exp(-E/R\ T_a)$. The Arrhenius constants (k_o) and activation energies (E) for influence of temperature on change in hardness are as follows:

$$\text{At } a_w = 0.30\text{: } k_o = 2.99 \times 10^{-1}\ /s\ ;\ r^2 = 0.974$$
$$E = 39.1\ kJ/mol$$
$$\text{At } a_w = 0.60\text{: } k_o = 1.47 \times 10^{-1}\ /s\ ;\ r^2 = 0.979$$
$$E = 34.4\ kJ/mol$$

Referring to Table 2.1, the positive activation energies for change in hardness show little resemblance to the negative activation energies characteristic of starch retrogradation. This supports the work of Kulp and Lorenz that states that no gelatinized starch is available for starch retrogradation and can not contribute to texture change in pastries. Activation energies for nonenzymatic browning are much higher than activation energies for change in hardness. But the activation energies for lipid oxidation (42 - 101 kJ/mol) are close to those for change in hardness. Knowledge of the oxygen permeabilities of the packaging materials used may be important if texture change is oxygen dependent. The influence of temperature on rate constants describing changes in cohesiveness and bending value are illustrated in Figures 5.11 and 5.12 respectively

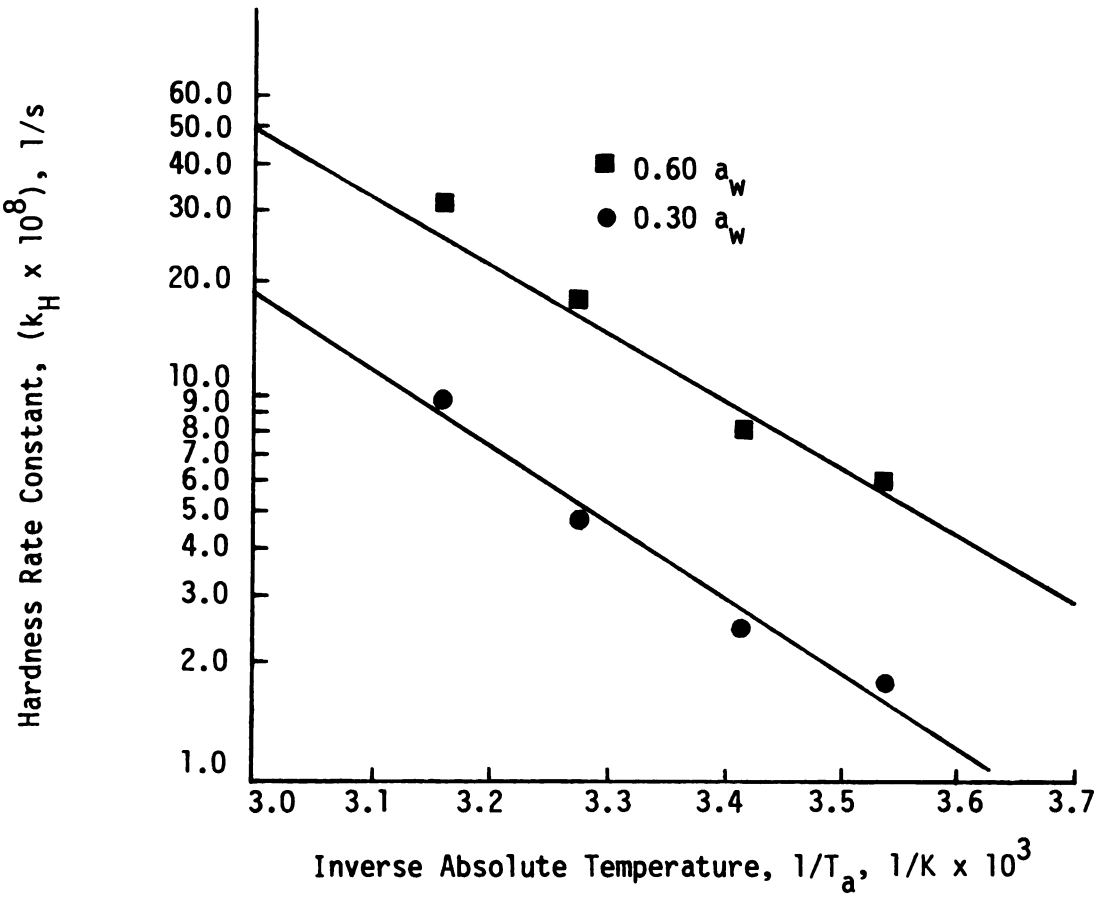

Figure 5.10 Arrhenius plot of first order rate constants for change in hardness at 0.30 and 0.60 water activity

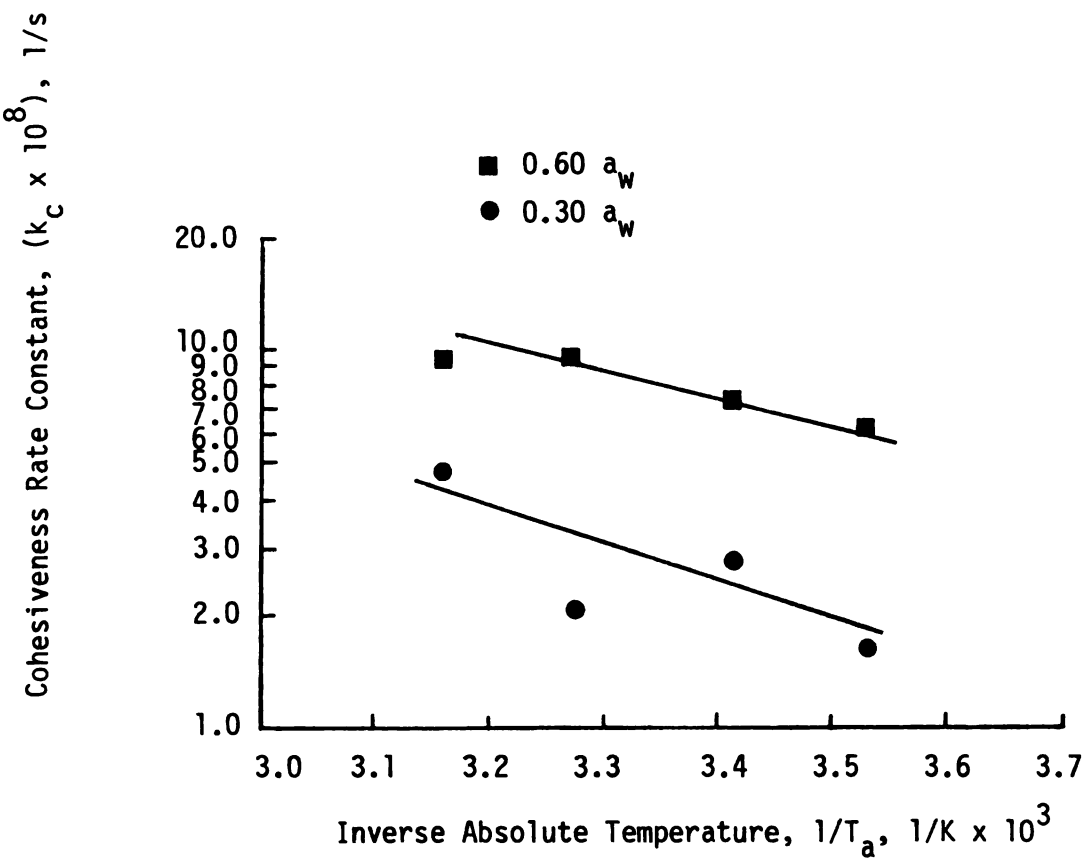

Figure 5.11 Arrhenius plot of first order rate constants for change in cohesiveness at 0.30 and 0.60 water activity

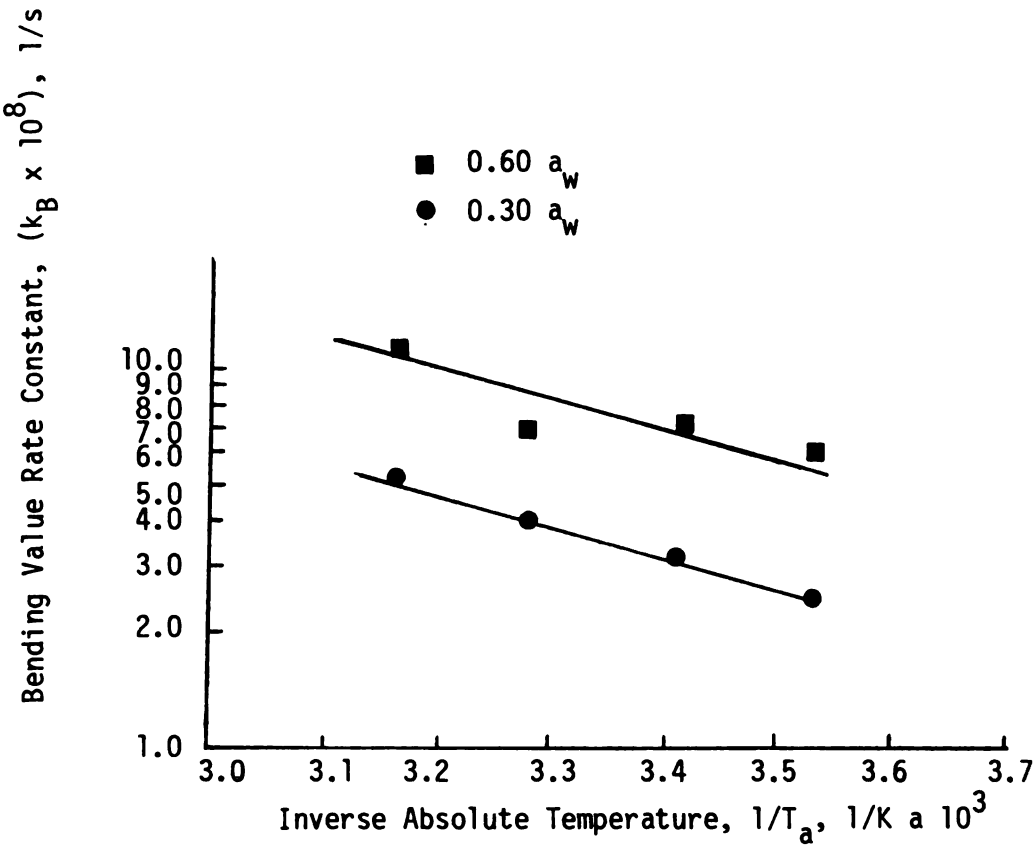

Figure 5.12 Arrhenius plot of first order rate constants for change in bending value at 0.30 and 0.60 water activity

where similar positive activation energies are evident as follows.

For cohesiveness:

At aw = 0.30: ko = 4.94 x 10-6 /s; r2 = 0.915

E = 9.95 kJ/mol

At aw = 0.60: ko = 1.46 x 10-1 /s; r2 = 0.718

E = 36.3 kJ/mol

For bending value:

At aw = 0.30: ko = 2.27 x 10-5 /s; r2 = 0.982

E = 15.7 kJ/mol

At aw = 0.60: ko = 9.29 x 10-6 /s; r2 = 0.719

E = 11.6 kJ/mol

5.7 Verification of Computer Prediction for Moisture Content

The results from the computer prediction, based on the model flow chart shown in Figure 3.1, and the experimental data for the moisture change in the sample during storage can be discussed in two parts, adsorption and desorption with examples shown in Figures 5.13 and 5.14 respectively. Because there was not sufficient data to generate Smith constants for adsorption, computer predictions were made for pastries stored at high relative humidities using desorption Smith constants. Though this is not standard practice, it was done here to illustrate the capabilities and shortcomings of the computer model. At conditions of 21 C

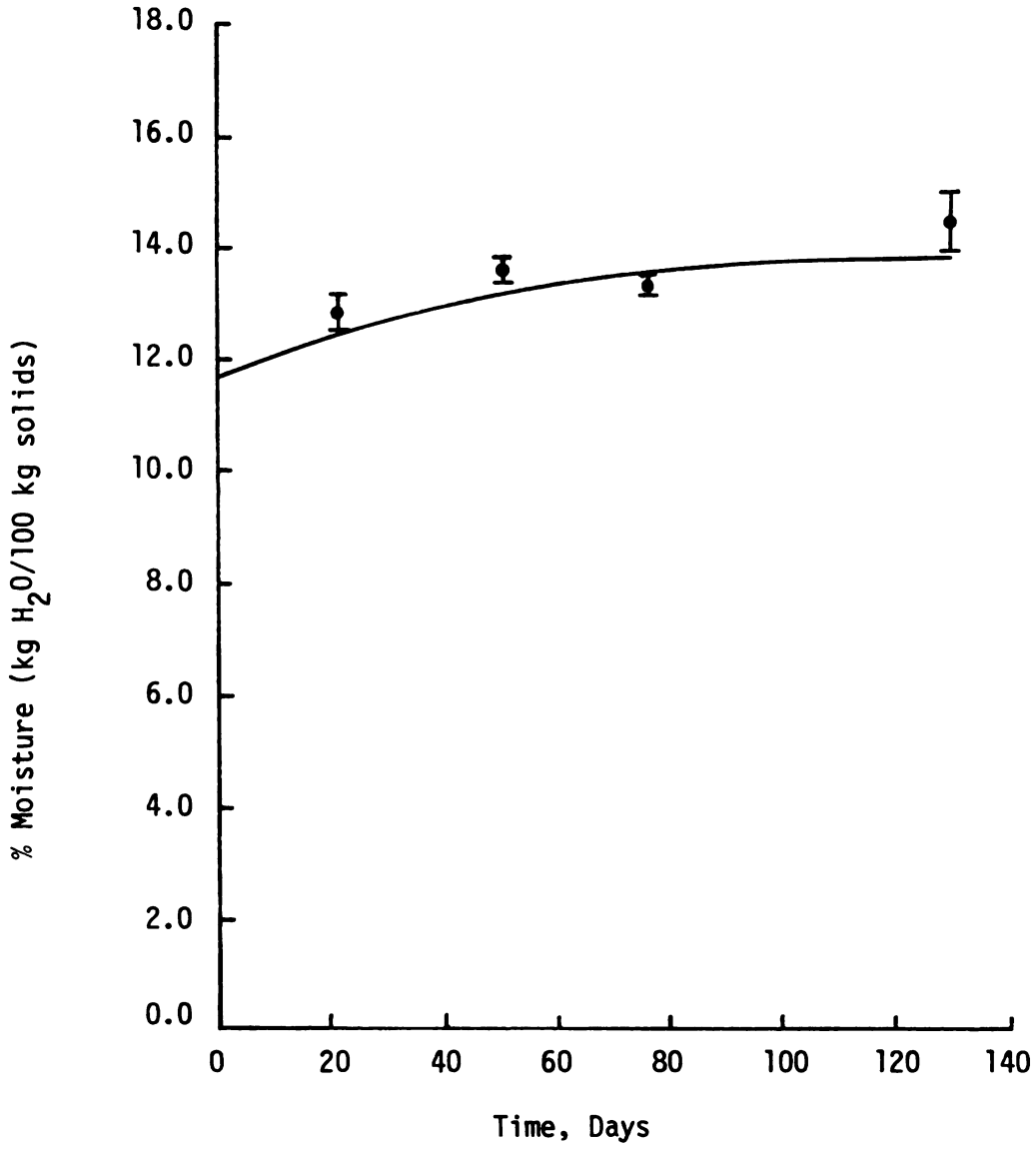

Figure 5.13 Comparison of experimental and computer predicted data for pastry moisture content during storage at 21 C and 76% RH in a polyethylene pouch

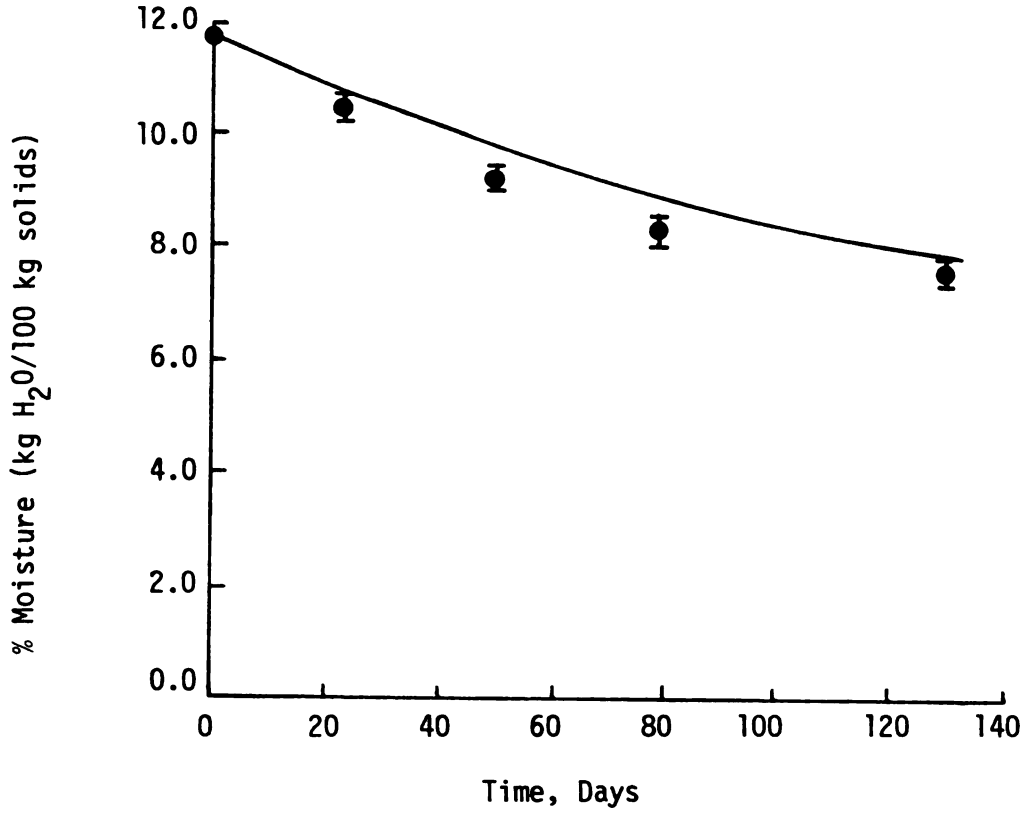

Figure 5.14 Comparison of experimental and computer predicted data for pastry moisture content during storage at 11 C and 37% RH in a polyethylene pouch

and 76% RH, and 21 C and 77% RH, the predicted adsorption of moisture in the model food system occurs because the storage water activities ($a_{w,o}$=RH/100) are higher than the initial water activities of the sample so moisture migrates from the environment into the product. On the other hand, at conditions of 11 C and 37% RH, 21 C and 35% RH, 22 C and 62% RH, 32 C and 42% RH, and 40 C and 40% RH, the predicted desorption of moisture from the model food system occurs because the storage water activities are lower than the initial water activities of the sample so moisture migrates from the product to the environment.

The averages of the percent differences between the predicted moisture content and experimental moisture contents are presented in Table 5.2. The computer predictions for the sample moisture content are in reasonable agreement with experimental data in all storage conditions except at the high water activities where desorption isotherm Smith constants were used for adsorption conditions. From a packaging perspective predictions of moisture content were just as effective for pastries in polyethylene pouches (permeability varies with temperature) as for polystyrene pouches (permeability remains constant with temperature). Deviations between the predicted and experimental data may be due to a number of other factors. Environmental conditions varied by standard deviations averaging 5.4% for temperature and 19.4% for relative humidity which may affect moisture sorption and rate of

Table 5.2 - Averages of absolute percent differences between computer predicted and experimentally derived moisture contents of pastries packaged in polyethylene and polystyrene pouches stored in seven different environments

		Average % Difference	
Temp, C	%RH	Polyethylene	Polystyrene
11	37	4.45	3.37
21	35	6.60	9.08
22	62	3.03	10.41
21	76	2.17	3.70
21	77	3.77	11.55
32	42	5.84	5.14
40	40	22.92	3.60

reaction significantly. Package sizes varied by standard deviations averaging 1.9% for polyethylene pouches and 2.7% for polystyrene pouches. This variation causes a proportional variation in the amount of water that permeates through the packaging material. Initial pastry weights varied by a standard deviation of 6.1%. For constant initial percent moistures and package areas, moisture contents and water activities would change more rapidly for smaller pastries than for larger ones.

5.8 Verification of Computer Prediction for Texture

The prediction model as shown in Figure 3.1 was used to predict the hardness of the pastries held in constant temperature and relative humidity environments and packaged in polyethylene, polystyrene, and foil pouches.

Predicted hardness values were compared with experimental values at storage conditions of 11 C and 37% RH, 21 C and 35% RH, 22 C and 62% RH, 21 C and 76% RH, 21 C and 77% RH, 32 C and 42% RH, and 40 C and 40% RH. For polyethylene, polystyrene, and foil pouches, the average of the percent differences between the predicted and experimental hardness values are presented in Table 5.3. Hardness values were consistently predicted at lower values than actual. More accurate predictions were made for pastries that experienced desorption in lower humidity environments than for pastries that experienced adsorption in higher humidity environments. This may be due to the

Table 5.3 - Averages of absolute percent differences between computer predicted and experimentally derived hardness values of pastries packaged in polyethylene, polystyrene, and foil pouches stored in seven different environments

		Average % Difference		
Temp, C	%RH	Polyethylene	Polystyrene	Foil Pouch
11	37	39.9	6.9	18.4
21	35	18.1	5.2	8.5
22	62	33.3	11.6	16.9
21	76	130.8	26.1	18.7
21	77	444.8	99.1	21.4
32	42	65.6	22.0	58.0
40	40	31.8	37.3	188.0

isotherm models inability to predict moisture contents at those conditions as well. The large 444.8% difference between predicted and actual values for pastries in the foil pouch at 40 C and 40% RH is not attributable to poor seals in the packaging material because actual values would probably be larger than predicted values. This discrepancy is not readily explained.

Experimental and computer predicted values for hardness are plotted in Figure 5.15 for the storage condition of 21 C and 35% RH in polystyrene packaging. At these conditions, there is a rapid loss of moisture and a corresponding increase in hardness primarily as a function of moisture loss. As moisture loss slows, the change in hardness due to chemical reaction predominates and the pastry becomes even harder. In foil pouch material, where there is no exchange of moisture with the environment, the change in hardness due to chemical reaction is the only mechanism responsible for change in hardness. In Figure 5.16, the experimental and predicted values for hardness, stored in a foil pouch, are compared at environmental conditions other than those used in the study with foil pouches to derive rate constants.

Figure 5.17 illustrates the interesting phenomenon that occurs with the pastries over time regardless of packaging materials. Though predicted values for texture keep rising, experimental results indicate that a maximum hardness is reached and hardness then begins to decrease. This maximum tends to be reached more quickly at higher temperatures and

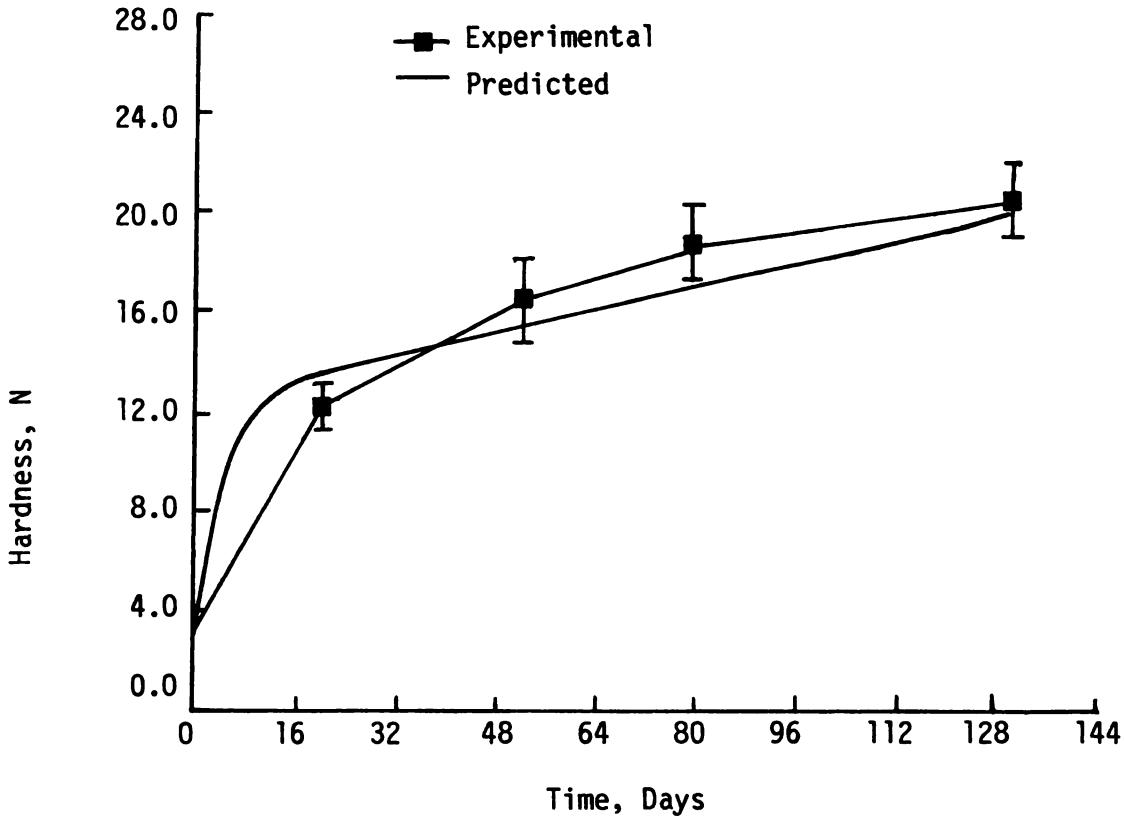

Figure 5.15 Comparison of experimental and computer predicted data for pastry hardness during storage at 21 C and 35% RH in a polystyrene pouch

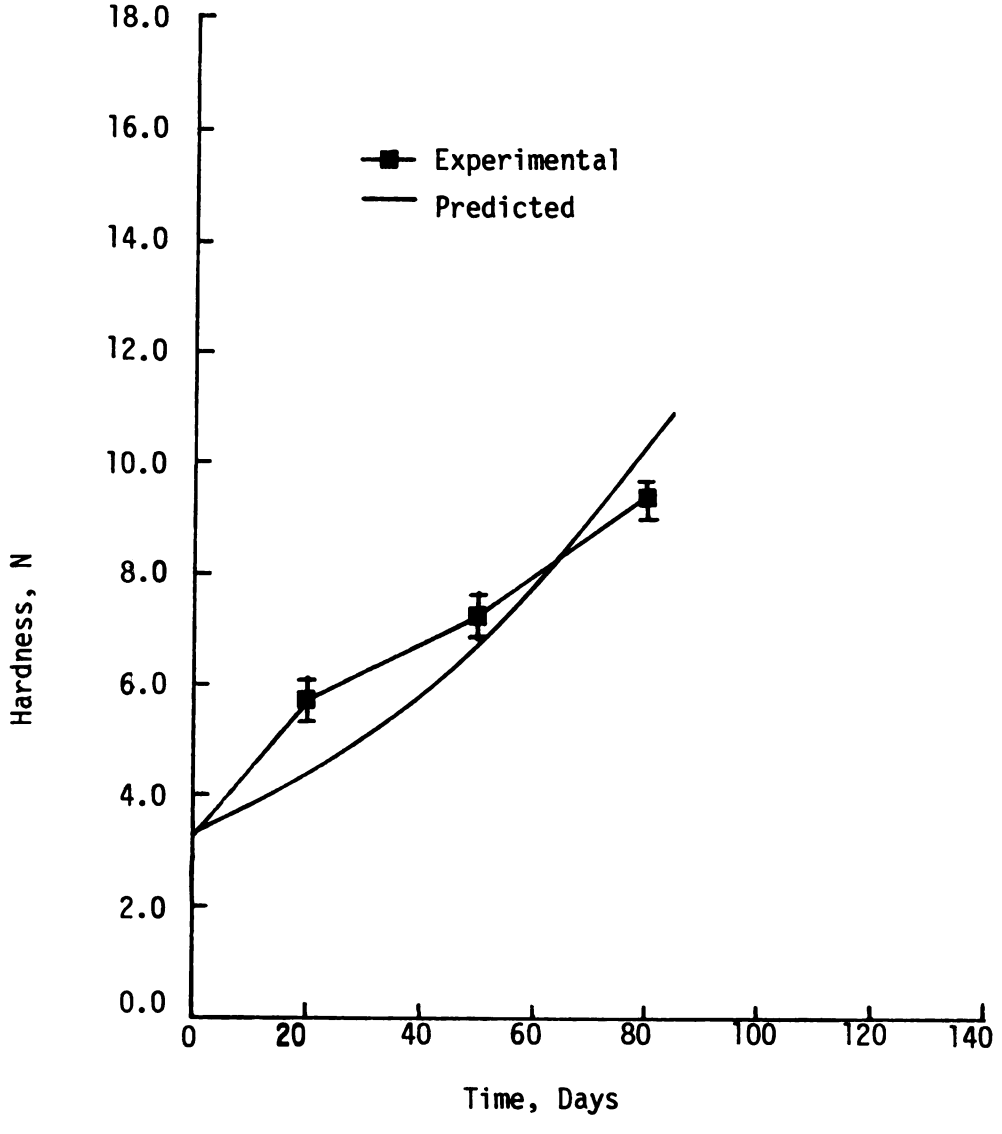

Figure 5.16 Comparison of experimental and computer-predicted data for pastry hardness during storage at 21 C in a foil pouch

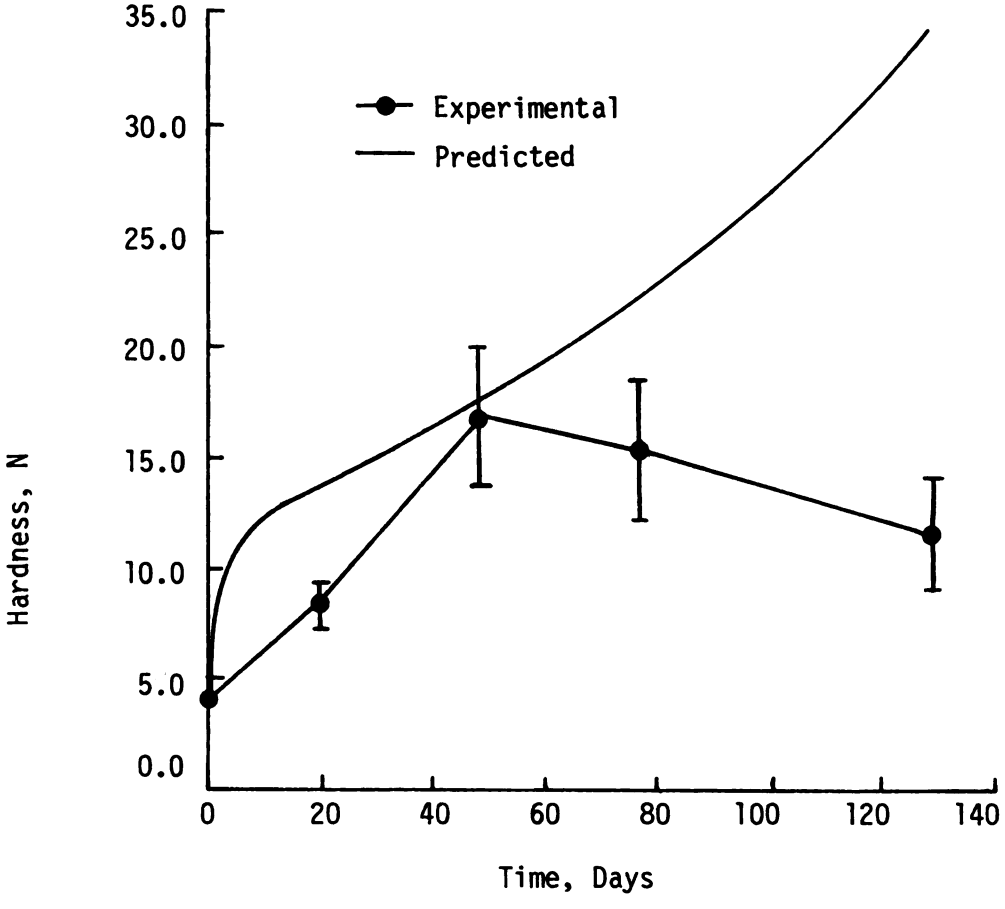

Figure 5.17 Comparison of experimental and computer predicted data for pastry hardness during storage at 32 C and 42% RH in a polystyrene pouch

water activities as evidenced in the data in Table A.5. Maximums are reached in 6 to 12 days at temperatures of 43 C, 15 to 32 days at 32 C, 53 days at 20 C and 0.73 water activity, and not reached at all within the time restraints of the experiment at 10 C and water activities below 0.73 at 20 C. This phenomenon was unexpected but with more extensive data, rate constants could be obtained on the downward trend of hardness with time. Similar maximums were observed for bending values and minimums for cohesiveness values over time as seen in Tables A.6 and A.7 respectively. The percent differences between experimental and computer predicted hardness values reported in Table 5.3 reflect only the data before the maximums were reached. The phenomenon may be due to breakdown of the insoluble protein and/or starch matrices over time due to some type of degradative mechanism. It may also be due to a change in the types of chemical reactions occurring within the pastry, due to a depletion of the chemical species responsible for change in texture.

VI. CONCLUSION

1. Initial hardness as a function of water activity can be described by an inverse linear relationship. Initial cohesiveness was found to increase with increasing water activity and initial bending values decreased with increasing water activity.

2. Experimental results at constant temperature and water activity indicate that rate of change in texture of a pastry based on hardness, cohesiveness, and bending value can be described by first order kinetics.

3. The rate constant for hardness change in pastries as a function of water activity can be described by an exponential relationship. Rate constants for cohesiveness change could not be described mathematically as a function of water activity consistently over a range of temperatures. Rate constants for change in bending value did increase with increasing water activities.

4. The rate constants for hardness change and in pastries as a function of temperature can be described by the Arrhenius relationship. The same was true for rate constants for cohesiveness and bending value change though correlation coefficients were lower than for the hardness relationships.

5. The computer predictions of moisture content in pastries over time are within 11.55 % of experimental moisture content data for temperatures ranging from 11 C to 32 C and relative humidities ranging from 35% RH to 77% RH in polyethylene and polystyrene packages (See Table 5.2).

6. The computer predictions of texture for pastries as described by hardness were predicted 6.9% to 65.6% lower than the experimental data for most conditions at relative humidities ranging from 35% RH to 62% RH, and temperatures between 11 C and 32 C in polyethylene and polystyrene pouches (See Table 5.3). These predictions were in agreement only to the extent where hardness values continued to increase and not become softer due to the phenomenon described in Section 5.8 for hardness values decreasing after a certain period of time.

7. Based on the experimental data, hardness was found to decrease after increasing for a period of time. This phenomenon tended to occur more rapidly at higher temperatures and relative humidities. Similar phenomenon occurred with bending values decreasing and cohesiveness increasing near the same time that hardness decreased.

6.1 Suggestions for Future Research

1. To monitor water activity of the pastry inside the package as well as moisture to make sure that isotherms are not shifting during storage due to chemical changes in the product.

2. To identify the mechanism responsible for texture change over time in pastries and other dry foods.

3. To identify the mechanism responsible for decrease in hardness after extended periods of storage.

4. To develop a model that will determine the influence of moisture migration from other food components as well as from the environment.

5. To verify experimentally the above model by incorporating other components, such as jams, jellies, nuts, glazes, etc. into the model food system.

6. To modify the computer model in this study to account for changing environmental conditions and verify it experimentally.

APPENDIX

APPENDIX A

TABLES

Table A.1 - Sorption isotherm data and Smith constants at 10 , 20, 32, and 43 C

10 C			20 C			32 C			43 C		
a_w	M	sdev	a_w	M	sdev	a_w	M	sdev	a_w	M	sdev
			0.18	4.20	0.19	0.21	3.42	0.19			
0.33	5.81	0.09	0.30	5.19	0.27	0.30	4.11	0.21	0.30	2.93	0.17
			0.44	6.15	0.18	0.45	5.40	0.15			
0.60	10.32	0.12	0.60	9.64	0.13	0.60	8.37	0.22	0.60	8.12	0.13
			0.73	14.20	0.50	0.74	13.93	0.31			

$$M = b \ln(1 - a_w) + a$$

a = 2.30	a = 1.78	a = 0.60	a = -0.38
b = -8.78	b = -9.09	b = -9.32	b = -9.27
r^2 = 1.00	r^2 = 0.98	r^2 = 0.97	r^2 = 1.00

$b = -8.04\ T\ \exp(0.040)$ $\quad r_2^2 = 0.93$

$a = -0.0817\ T + 3.23$ $\quad r^2 = 0.99$

Table A.2 - Initial hardness at experimental equilibrium water activities and temperatures

10 C		20 C		32 C		43 C	
H_o	std dev	H_o	std dev	H_o	std dev	H_o	std dev
		a_w = 0.18		a_w = 0.21			
		12.1	1.9	11.1	0.8		
a_w = 0.33		a_w = 0.30		a_w = 0.30		a_w = 0.30	
12.6	2.4	13.4	0.7	14.3	2.2	14.6	1.4
		a_w = 0.44		a_w = 0.45			
		10.1	0.6	10.8	0.7		
a_w = 0.60		a_w = 0.60		a_w = 0.60		a_w = 0.60	
4.23	0.44	4.41	0.4	1.53	0.33	7.56	0.98
		a_w = 0.73		a_w = 0.74			
		1.53	0.33	2.39	0.3		

$$H_o = M_a + M_b(a_w)$$

M_a = 22.8	M_a = 22.2	M_a = 22.7	M_a = 21.8
M_b^a = -31.0	M_b^a = -28.6	M_b^a = -26.7	M_b^a = -23.8
	r^2 = 0.991	r^2 = 0.993	

Table A.3 - Initial cohesiveness at experimental equilibrium water activities and temperatures

10 C		20 C		32 C		43 C	
C_o	std dev	C_o	std dev	C_o	std dev	C_o	std dev
		a_w = 0.18		a_w = 0.21			
		0.081	0.033	0.109	0.016		
a_w = 0.33		a_w = 0.30		a_w = 0.30		a_w = 0.30	
0.091	0.012	0.075	0.017	0.147	0.023	0.201	0.024
		a_w = 0.44		a_w = 0.45			
		0.195	0.038	0.299	0.027		
a_w = 0.60		a_w = 0.60		a_w = 0.60		a_w = 0.60	
0.317	0.021	0.411	0.024	0.393	0.022	0.427	0.022
		a_w = 0.73		a_w = 0.74			
		0.443	0.016	0.443	0.024		

Table A.4 - Initial bending value at experimental equilibrium water activities and temperatures

10 C		20 C		32 C		43 C	
B_ox100	std dev	B_ox100	std dev	B_ox100	std dev	B_ox100	std dev
		a_w = 0.18		a_w = 0.21			
		14.4	0.6	16.1	0.7		
a_w = 0.33		a_w = 0.30		a_w = 0.30		a_w = 0.30	
14.9	0.3	15.7	0.4	16.6	0.6	17.5	0.4
		a_w = 0.44		a_w = 0.45			
		9.92	1.59	10.2	0.5		
a_w = 0.60		a_w = 0.60		a_w = 0.60		a_w = 0.60	
4.09	0.32	4.39	0.46	5.06	0.43	5.83	0.45
		a_w = 0.73		a_w = 0.74			
		2.02	0.12	1.66	0.15		

Table A.5 - Hardness vs. time at experimental equilibrium water activities and temperatures

10 C			20 C			32 C			43 C		
Time, days	H	std dev	Time, days	H	std dev	Time, days	H	std dev	Time, days	H	std dev
			a_w = 0.18			a_w = 0.21					
			0	12.1	1.9	0	11.1	0.8			
			37	13.0	1.3	26	12.1	2.0			
			59	13.7	2.0	32	12.4	3.1			
			76	15.6	2.5	42	11.9	2.3			
a_w = 0.33			a_w = 0.30			a_w = 0.30			a_w = 0.30		
0	12.5	2.4	0	13.4	0.7	0	14.3	2.2	0	14.6	1.4
17	13.0	2.0	45	15.2	0.1	20	16.1	0.8	12	16.5	1.1
34	13.3	0.9	68	15.8	0.9	36	17.1	1.6	21	15.8	1.6
			81	16.5	0.9	46	16.1	1.1			
			a_w = 0.44			a_w = 0.45					
			0	10.1	0.6	0	10.8	0.7			
			26	11.4	0.7	14	12.5	0.5			
			48	12.6	0.4	30	14.6	0.5			
			70	14.3	0.4	40	13.7	0.6			
a_w = 0.60			a_w = 0.60			a_w = 0.60			a_w = 0.60		
0	4.26	0.44	0	4.41	0.40	0	7.21	1.89	0	7.56	0.98
12	4.55	1.44	29	5.56	0.47	21	10.5	0.9	6	8.83	0.86
28	4.88	0.55	53	6.68	0.45	26	9.84	0.68	16	8.62	0.92
40	5.41	0.44	67	7.58	0.43	37	8.65	1.06			
			a_w = 0.73			a_w = 0.74					
			0	1.53	0.33	0	2.39	0.30			
			22	1.99	0.46	15	3.92	0.29			
			53	2.94	0.34	32	3.63	0.49			
			77	1.56	0.26	46	2.40	0.24			

Table A.6 - Cohesiveness vs. time at experimental equilibrium water activities and temperatures

10 C			20 C			32 C			43 C		
Time, days	C	std dev	Time, days	C	std dev	Time, days	C	std dev	Time, days	C	std dev
				a_w = 0.18			a_w = 0.21				
			0	0.081	0.033	0	0.109	0.016			
			37	0.106	0.015	26	0.115	0.026			
			59	0.125	0.021	32	0.144	0.027			
			76	0.136	0.023	42	0.124	0.025			
	a_w = 0.33			a_w = 0.30			a_w = 0.30			a_w = 0.30	
0	0.091	0.012	0	0.075	0.017	0	0.147	0.023	0	0.201	0.024
17	0.101	0.010	45	0.091	0.015	20	0.147	0.029	12	0.224	0.025
34	0.112	0.014	68	0.109	0.017	36	0.200	0.022	21	0.194	0.023
			81	0.133	0.021	46	0.189	0.018			
				a_w = 0.44			a_w = 0.45				
			0	0.195	0.038	0	0.299	0.027			
			26	0.255	0.035	14	0.370	0.038			
			48	0.267	0.039	30	0.421	0.028			
			70	0.282	0.033	40	0.397	0.026			
	a_w = 0.60			a_w = 0.60			a_w = 0.60			a_w = 0.60	
0	0.317	0.021	0	0.411	0.024	0	0.393	0.022	0	0.427	0.022
12	0.324	0.016	29	0.426	0.032	21	0.402	0.015	6	0.439	0.019
28	0.333	0.019	53	0.430	0.022	26	0.395	0.019	16	0.401	0.019
40	0.339	0.013	67	0.498	0.014	37	0.390	0.011			
				a_w = 0.73			a_w = 0.74				
			0	0.443	0.016	0	0.443	0.024			
			22	0.493	0.018	15	0.540	0.032			
			53	0.512	0.032	32	0.502	0.011			
			77	0.464	0.011	46	0.462	0.020			

Table A.7 - Bending value vs. time at experimental equilibrium water activities and temperatures

10 C			20 C			32 C			43 C		
Time, days	Bx100	std dev	Time, days	Bx100	std dev	Time, days	Bx100	std dev	Time, days	Bx100	std dev
			a_w = 0.18			a_w = 0.21					
			0	14.4	0.6	0	16.1	0.7			
			37	18.1	0.8	26	18.1	0.7			
			59	19.8	0.4	32	19.3	0.7			
			76	20.1	0.7	42	19.9	0.6			
a_w = 0.33			a_w = 0.30			a_w = 0.30			a_w = 0.30		
0	14.9	0.3	0	15.7	0.4	0	16.6	0.6	0	17.5	0.4
17	15.6	0.5	45	16.3	0.5	20	18.5	0.5	12	18.6	0.5
34	16.2	0.4	68	19.4	0.4	36	19.0	0.5	21	18.0	0.4
			81	19.8	0.4	46	17.7	0.5			
			a_w = 0.44			a_w = 0.45					
			0	9.92	1.59	0	10.2	0.5			
			26	11.4	0.5	14	11.1	0.5			
			48	12.1	0.7	30	12.6	0.4			
			70	13.2	0.6	40	11.3	0.4			
a_w = 0.60			a_w = 0.60			a_w = 0.60			a_w = 0.60		
0	4.09	0.32	0	4.39	0.46	0	5.06	0.43	0	5.83	0.45
12	4.41	0.35	29	5.08	0.32	21	5.85	0.42	6	6.25	0.49
28	4.91	0.30	53	5.98	0.38	26	5.39	0.38	16	5.62	0.52
40	5.22	0.40	67	6.94	0.29	37	5.32	0.26			
			a_w = 0.73			a_w = 0.74					
			0	2.02	0.12	0	1.66	0.15			
			22	2.70	0.18	15	1.86	0.28			
			53	3.92	0.21	32	1.69	0.14			
			77	3.86	0.12	46	1.42	0.19			

Table A.8 - First order rate constants for change in hardness at experimental equilibrium water activities and temperatures

$k \times 10^8$, 1/s			
10 C	20 C	32 C	43 C
	a_w = 0.18 3.61	a_w = 0.21 3.99	
a_w = 0.33 2.03	a_w = 0.30 2.84	a_w = 0.30 5.52	a_w = 0.30 11.4
	a_w = 0.44 5.82	a_w = 0.45 11.7	
a_w = 0.60 6.74	a_w = 0.60 9.39	a_w = 0.60 20.4	a_w = 0.60 28.6
	a_w = 0.73 14.4	a_w = 0.74 37.7	

Table A.9 - First order rate constants for change in cohesiveness at experimental equilibrium water activities and temperatures

$k \times 10^8$, 1/s			
10 C	20 C	32 C	43 C
	a_w = 0.18 7.77	a_w = 0.21 8.16	
a_w = 0.33 7.03	a_w = 0.30 8.33	a_w = 0.30 10.6	a_w = 0.30 10.6
	a_w = 0.44 5.27	a_w = 0.45 12.7	
a_w = 0.60 1.89	a_w = 0.60 3.23	a_w = 0.60 1.15	a_w = 0.60 5.31
	a_w = 0.73 3.17	a_w = 0.74 15.2	

Table A.10 - First order rate constants for change in bending value at experimental equilibrium water activities and temperatures

$k \times 10^8$, 1/s			
10 C	20 C	32 C	43 C
	a_w = 0.18 5.16	a_w = 0.21 5.95	
a_w = 0.33 2.87	a_w = 0.30 3.67	a_w = 0.30 4.36	a_w = 0.30 5.94
	a_w = 0.44 4.31	a_w = 0.45 8.29	
a_w = 0.60 7.07	a_w = 0.60 8.34	a_w = 0.60 7.95	a_w = 0.60 12.9
	a_w = 0.73 14.4	a_w = 0.74 8.68	

Table A.11 - Physical data of pastries during storage in polystyrene, polyethylene, and foil pouches at 11 C and 37 % RH

$a = 2.33$ $\quad M_a = 22.4$
$b = -8.85$ $\quad M_b = -30.7$

Foil Pouch

time days	M	std dev	H	std dev	C	std dev	Bx100	std dev
23	11.82	---	4.7	0.4	0.44	0.04	3.1	0.4
49	"	---	4.8	0.3	0.44	0.04	3.2	0.4
79	"	---	5.0	0.4	0.42	0.03	3.7	1.6
130	"	---	5.6	0.4	0.44	0.02	3.2	0.6

Polyethylene

time days	M	std dev	H	std dev	C	std dev	Bx100	std dev
23	10.55	0.04	3.9	0.3	0.51	0.06	2.7	0.8
49	9.30	0.13	4.0	0.3	0.52	0.05	3.6	0.5
79	8.30	0.14	5.4	0.5	0.44	0.05	5.7	0.8
130	7.60	0.29	8.0	0.6	0.35	0.04	6.9	0.9

Polystyrene

time days	M	std dev	H	std dev	C	std dev	Bx100	std dev
23	7.10	0.14	10.7	0.8	0.29	0.04	6.5	0.9
49	6.42	0.19	12.1	1.1	0.35	0.03	8.1	1.0
79	6.33	0.66	12.6	0.9	0.28	0.03	10.3	0.3
130	6.97	0.29	13.5	1.6	0.25	0.03	10.3	2.9

Table A.12 - Physical data of pastries during storage in polystyrene, polyethylene, and foil pouches at 21 C and 35 % RH

$a = 1.54$ $\quad M_a = 22.4$
$b = -9.08$ $\quad M_b = -30.7$

Foil Pouch

time days	M	std dev	H	std dev	C	std dev	Bx100	std dev
20	11.82	---	5.6	0.2	0.46	0.04	2.5	1.3
50	"	---	7.1	0.9	0.41	0.04	3.6	0.2
79	"	---	9.3	0.6	0.41	0.03	4.5	0.8
130	"	---	6.9	1.1	0.39	0.03	6.1	1.0

Polyethylene

time days	M	std dev	H	std dev	C	std dev	Bx100	std dev
20	7.92	0.19	6.0	0.5	0.48	0.06	5.4	1.8
50	7.20	0.55	9.2	0.6	0.20	0.06	10.2	1.4
79	6.43	0.27	14.3	1.2	0.14	0.05	14.1	2.4
130	6.13	0.28	9.2	2.9	0.16	0.04	12.5	3.0

Polystyrene

time days	M	std dev	H	std dev	C	std dev	Bx100	std dev
20	5.54	0.27	12.3	1.0	0.19	0.03	11.7	3.9
50	5.44	0.08	16.4	1.8	0.19	0.06	10.2	0.1
79	4.47	0.55	18.7	1.5	0.14	0.04	12.9	3.6
130	4.46	0.29	20.2	1.6	0.13	0.04	14.9	1.4

Table A.13 - Physical data of pastries during storage in polystyrene, polyethylene, and foil pouches at 22 C and 62 % RH

$a = 1.46$ $\quad M_a = 22.4$
$b = -9.09$ $\quad M_b = -28.5$

Foil Pouch

time days	M	std dev	H	std dev	C	std dev	Bx100	std dev
21	11.82	---	3.8	0.4	0.48	0.04	4.1	1.2
50	"	---	5.4	1.0	0.46	0.02	4.8	1.1
79	"	---	5.6	2.0	0.50	0.03	5.2	1.4
130	"	---	5.5	2.4	0.42	0.03	5.1	1.0

Polyethylene

time days	M	std dev	H	std dev	C	std dev	Bx100	std dev
21	11.70	0.44	4.3	0.4	0.55	0.05	2.4	0.4
50	11.28	0.17	4.7	0.8	0.38	0.04	4.2	0.6
79	10.48	0.29	6.2	0.7	0.41	0.04	3.2	0.1
130	10.96	0.28	4.2	0.7	0.45	0.03	3.3	0.6

Polystyrene

time days	M	std dev	H	std dev	C	std dev	Bx100	std dev
21	9.14	0.70	4.8	0.4	0.48	0.03	4.2	0.8
50	7.68	0.29	8.7	1.8	0.36	0.05	5.4	0.8
79	10.08	0.22	6.9	2.6	0.47	0.03	2.5	0.7
130	10.67	0.82	3.2	0.8	0.51	0.03	4.7	3.3

Table A.14 - Physical data of pastries during storage in polystyrene, polyethylene, and foil pouches at 21 C and 76 % RH

$a = 1.53$ $\quad M_a = 22.4$
$b = -9.08$ $\quad M_b = -28.7$

Foil Pouch

time days	M	std dev	H	std dev	C	std dev	Bx100	std dev
21	11.82	---	4.6	0.2	0.45	0.06	5.5	1.3
50	"	---	5.5	0.3	0.44	0.02	3.8	0.6
78	"	---	6.6	1.8	0.43	0.03	6.8	1.7
130	"	---	6.3	2.0	0.46	0.04	3.2	0.1

Polyethylene

time days	M	std dev	H	std dev	C	std dev	Bx100	std dev
21	12.93	0.34	2.3	0.1	0.61	0.04	2.4	0.2
50	13.56	0.08	2.2	0.3	0.54	0.03	2.0	0.6
78	13.42	0.09	1.9	0.8	0.52	0.02	2.0	0.3
130	14.42	0.64	2.4	0.4	0.50	0.02	2.2	0.1

Polystyrene

time days	M	std dev	H	std dev	C	std dev	Bx100	std dev
21	14.56	0.17	1.7	0.2	0.66	0.06	2.0	0.5
50	14.21	0.25	2.1	0.6	0.55	0.03	1.9	0.7
78	14.96	0.24	1.5	0.5	0.55	0.03	1.4	0.3
130	15.99	0.53	0.9	0.2	0.56	0.04	1.6	0.3

Table A.15 - Physical data of pastries during storage in polystyrene, polyethylene, and foil pouches at 21 C and 77 % RH

$a = 1.49$ $M_a = 22.4$
$b = -9.09$ $M_b = -28.6$

Foil Pouch

time days	M	std dev	H	std dev	C	std dev	Bx100	std dev
20	11.82	---	5.0	0.2	0.44	0.01	4.6	0.1
49	"	---	5.7	0.9	0.43	0.03	4.0	0.3
78	"	---	6.6	0.6	0.46	0.03	4.8	0.4
128	"	---	5.4	1.8	0.42	0.02	4.6	0.4

Polyethylene

time days	M	std dev	H	std dev	C	std dev	Bx100	std dev
20	12.09	0.07	3.6	0.3	0.57	0.06	2.3	0.3
49	12.78	0.28	3.0	0.4	0.52	0.04	2.5	0.7
78	13.40	0.23	1.4	0.5	0.52	0.03	1.8	0.1
128	15.46	0.39	1.3	0.3	0.52	0.03	1.4	0.2

Polystyrene

time days	M	std dev	H	std dev	C	std dev	Bx100	std dev
20	11.19	0.29	3.3	0.3	0.58	0.08	3.4	0.6
49	13.68	0.65	2.1	0.6	0.57	0.04	2.2	0.4
78	15.89	0.53	1.2	0.3	0.54	0.03	1.0	0.3

Table A.16 - Physical data of pastries during storage in polystyrene, polyethylene, and foil pouches at 32 C and 42 % RH

$a = 0.58$ $\quad M_a = 22.4$

$b = -9.24$ $\quad M_b = -26.3$

Foil Pouch

time days	M	std dev	H	std dev	C	std dev	Bx100	std dev
20	11.82	---	5.5	0.6	0.49	0.03	8.0	0.8
49	"	---	5.8	0.7	0.46	0.04	3.0	0.3
77	"	---	3.2	0.8	0.46	0.03	2.5	0.5
128	"	---	2.9	1.5	0.46	0.04	2.4	0.7

Polyethylene

time days	M	std dev	H	std dev	C	std dev	Bx100	std dev
20	6.94	0.49	7.0	0.6	0.31	0.05	20.0	4.2
49	6.72	0.83	9.6	1.0	0.20	0.04	9.0	3.8
77	5.93	0.47	12.4	1.8	0.18	0.03	9.2	2.6
128	5.59	0.53	10.1	3.1	0.18	0.05	7.3	0.8

Polystyrene

time days	M	std dev	H	std dev	C	std dev	Bx100	std dev
20	5.65	0.62	8.4	0.9	0.34	0.06	6.6	1.2
49	5.79	0.28	17.0	2.6	0.18	0.03	25.1	6.7
77	4.82	0.53	15.1	2.8	0.22	0.03	9.2	3.7
130	4.75	0.41	11.3	2.0	0.26	0.04	7.5	0.9

Table A.17 - Physical data of pastries during storage in polystyrene, polyethylene, and foil pouches at 43 C and 40 % RH

$a = -0.03$ $\quad M_a = 22.4$

$b = -9.32$ $\quad M_b = -24.7$

Foil Pouch

time days	M	std dev	H	std dev	C	std dev	Bx100	std dev
19	11.82	---	4.8	0.5	0.44	0.06	4.7	1.7
48	"	---	6.3	0.5	0.38	0.02	5.5	1.4
77	"	---	2.7	0.6	0.53	0.03	3.3	0.4
128	"	---	2.7	1.3	0.48	0.01	2.4	1.5

Polyethylene

time days	M	std dev	H	std dev	C	std dev	Bx100	std dev
19	8.37	0.92	11.0	0.8	0.10	0.04	14.2	1.2
48	6.65	0.90	8.8	2.0	0.23	0.05	10.1	3.6
77	6.71	0.53	7.1	1.4	0.31	0.04	8.2	2.9
128	5.51	0.94	7.2	2.0	0.16	0.03	8.7	2.0

Polystyrene

time days	M	std dev	H	std dev	C	std dev	Bx100	std dev
19	5.61	0.36	11.3	0.7	0.19	0.04	13.2	0.1
48	5.59	0.40	10.7	1.6	0.14	0.03	11.1	1.4
77	4.94	0.54	10.1	2.0	0.13	0.03	9.6	1.7
128	3.67	0.31	10.2	2.2	0.29	0.05	8.4	2.2

APPENDIX B

FIGURES

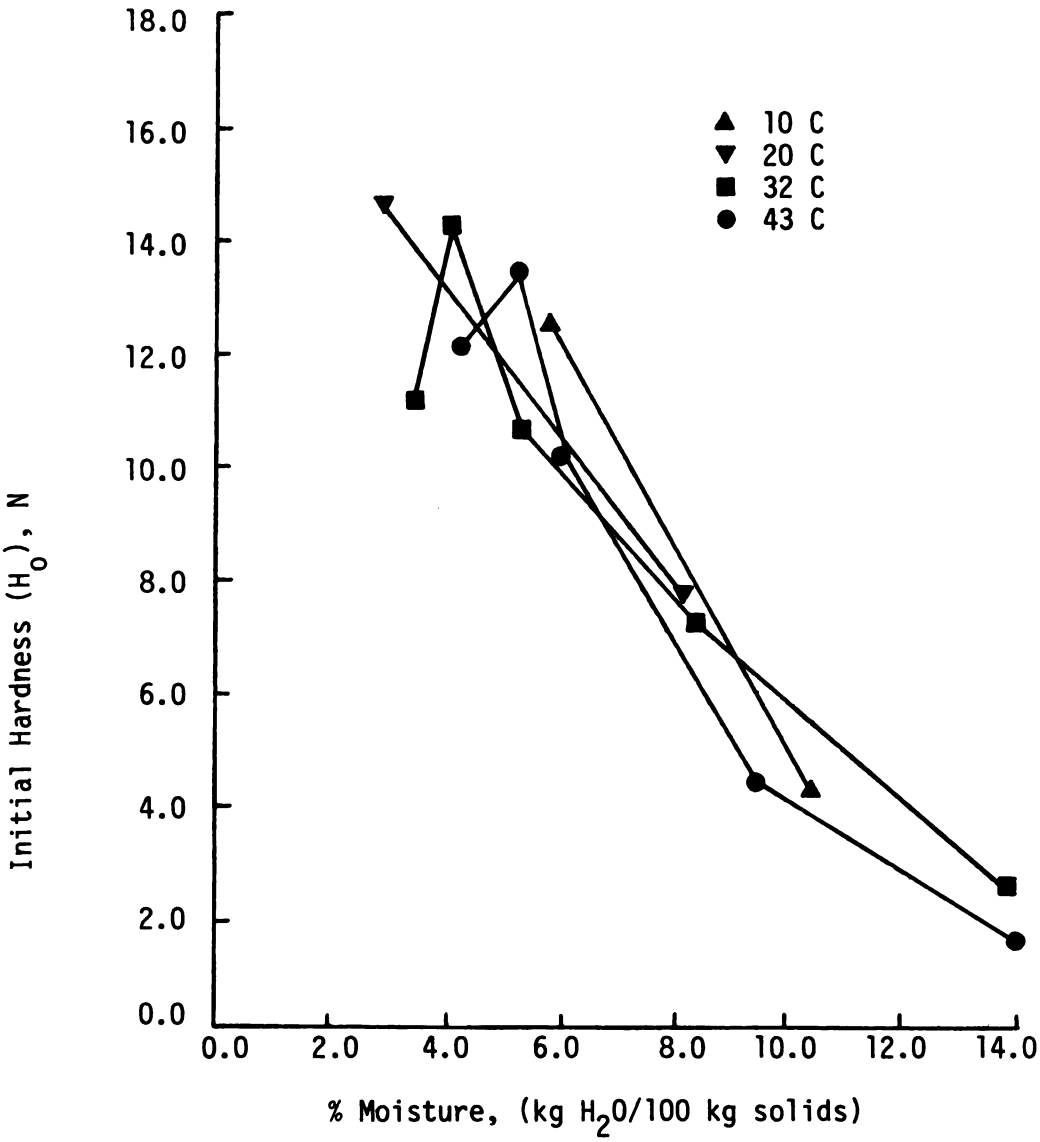

Figure B.1 Initial hardness vs. % moisture at 10, 20, 32, and 43 C

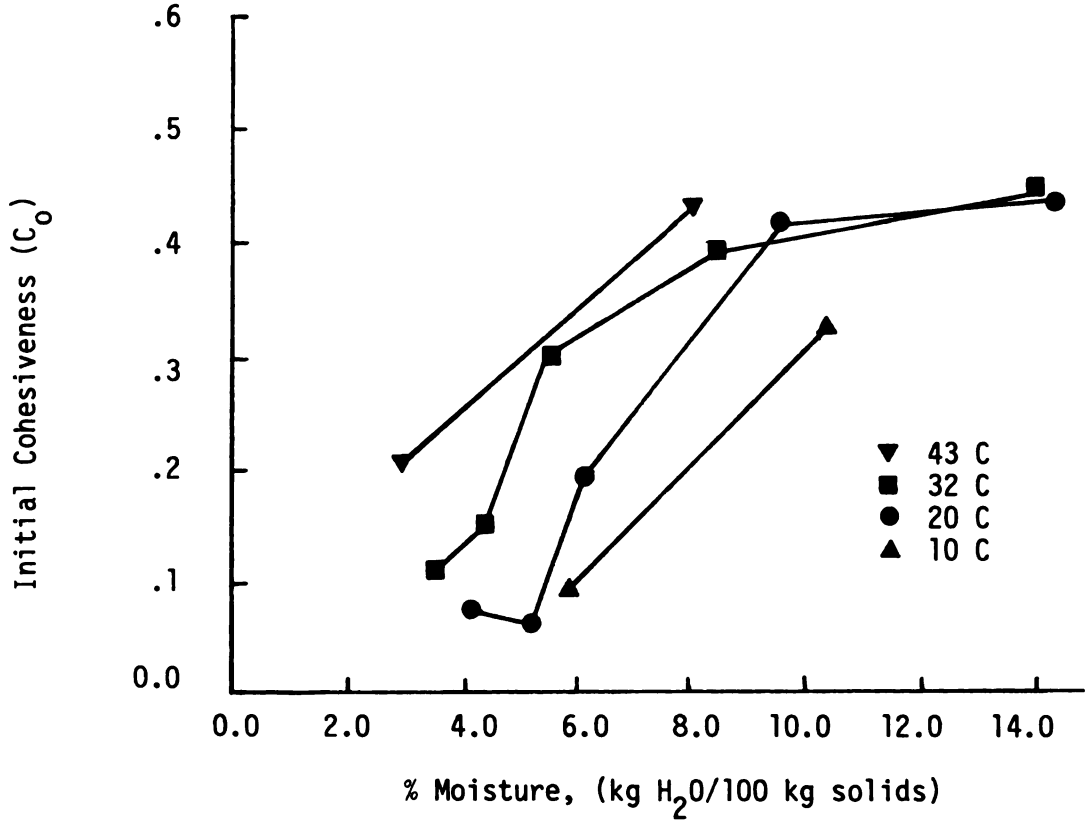

Figure B.2 Initial cohesiveness vs. % moisture at 10, 20, 32, and 43 C

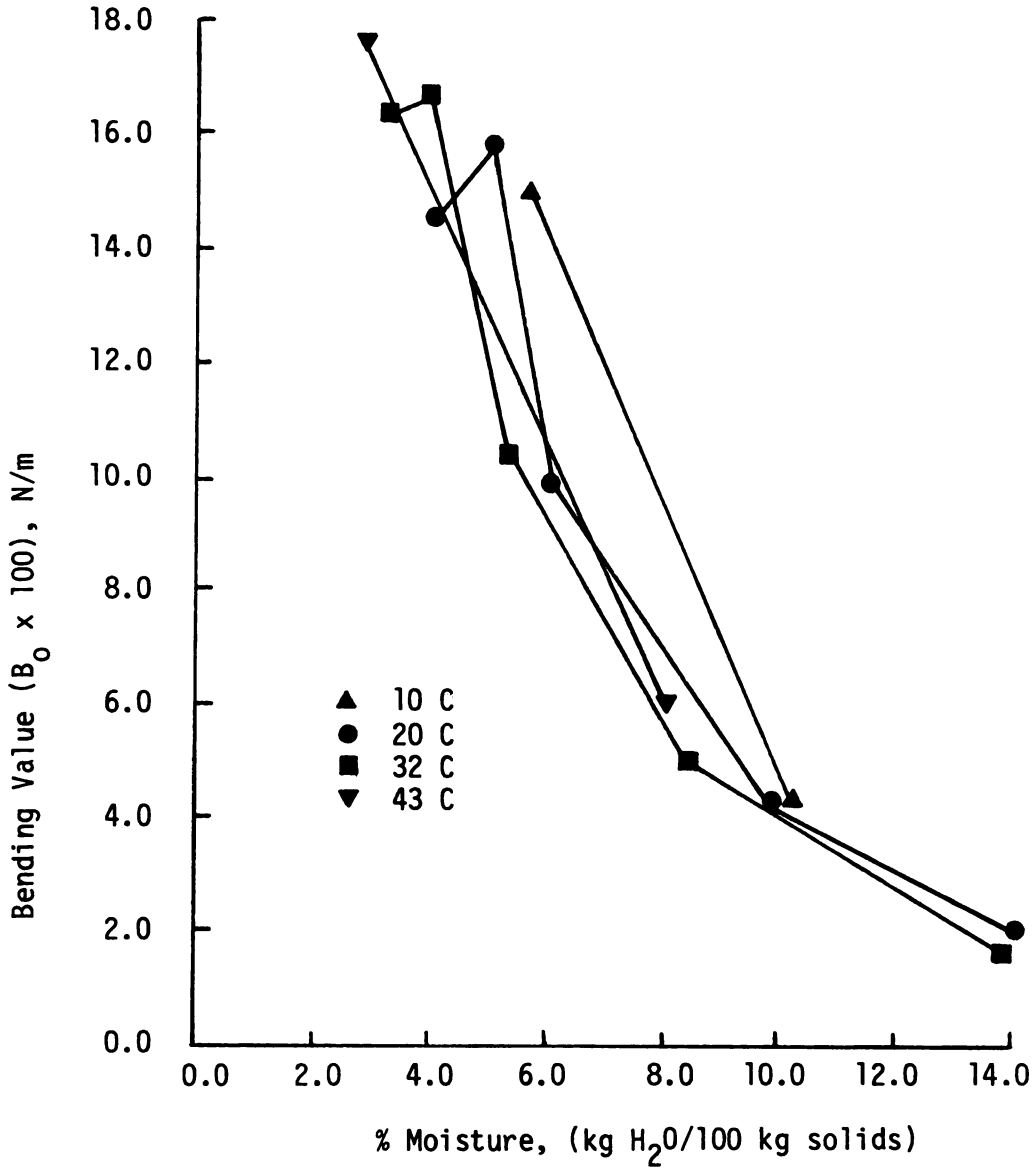

Figure B.3 Initial bending value vs. % moisture at 10, 20, 32, and 43 C

APPENDIX C

COMPUTER PROGRAM LISTING

```
 10 DEFDBL A-Z
 20 CLS:CLOSE:Z=2
 30 OPEN "scrn:" FOR OUTPUT AS #2
 40 PRINT "%RH OUTSIDE; TEMPERATURE,C"
 50 INPUT RHOUT,TEMPC
 60 PRINT "ISOTHERM: SMITHa, SMITHb"
 70 INPUT IA,IB
 80 PRINT "MOISTURE EFECT: Ma, Mb"
 90 INPUT MEA,MEB
100 PRINT "INITIAL TEXTURE"
110 INPUT TEXO
120 PRINT "TEXTURE CHANGE RATE: KA, KB"
130 INPUT TEXRA,TEXRB
140 PRINT "PRODUCT WT, G; INITIAL %M, G/100G"
150 INPUT PRODWTG,H2OPDBI
160 PRINT "PACKAGE AREA, CM2;THICKNESS, MIL"
170 INPUT AREACM2,THICKNESSMIL
180 PRINT "FILM PERMEABILITY CONSTANT, KG*M/M2*S*PA"
190 INPUT PCONST
200 PRINT "STORAGE TIME, DAYS; DISPLAY INCREMENT, DAYS; TIME
    INCREMENT, HRS"
210 INPUT STORTIMEDAY,DISPINCDAY,TIMEINCHR
220 ER=-36150!/8.31441:K=273.15:TR=32.2:TA=-1/(K+TR)
230 THICKNESSM=.0000254*THICKNESSMIL
240 VP1=1.40974E+10:VP2=-3928.5:VP3=231.667
250 TIMEINCSEC=TIMEINCHR*3600:TIMEINCDAY=TIMEINCHR/24
260 DISPCNT=0:STORCNT=0
270 H2OPDB=H2OPDBI: H2ODDB = H2OPDB/100: H2ODWB =
    H2ODDB/(1+H2ODDB)
280 SOLIDSG=PRODWTG-PRODWG*H2ODWB
290 AWIN1=1-EXP((H2OPDB-IA)/IB)
300 TEX=TEXO
310 PRINT #Z,
320 PRINT #Z,;"*****************************************"
330 PRINT #Z,
340 PRINT #Z,;"    OUTSIDE %RH = ";RHOUT
350 PRINT #Z,;"        TEMP, C = ";TEMPC
360 PRINT #Z,;"        SMITH,A = ";IA
370 PRINT #Z,;"        SMITH,B = ";IB
380 PRINT #Z,;"             MA = ";MEA
390 PRINT #Z,;"             MB = ";MEB
400 PRINT #Z,;"             KA = ";TEXRA
410 PRINT #Z,;"             KB = ";TEXRB
420 PRINT #Z,;" PRODUCT WT., G = ";PRODWTG
430 PRINT #Z,;"   %MDB, G/100G = ";H2OPDB
440 PRINT #Z,;"       AREA, CM2 = ";AREACM2
450 PRINT #Z,;" Thickness, mil = ";THICKNESSMIL
460 PRINT #Z,;" P,KG*M/M2*S*PA = ";PCONST
470 PRINT #Z,;"         DT, HR = ";TIMEINCHR
480 PRINT #Z,:PRINT #Z,
490 PRINT #Z,; "DAYS"; TAB(7); "AW"; TAB(12); "%MDB";
    TAB(18); "TEXTURE";TAB(28);"TEX RATE"
500 PRINT #Z,;"---- ----- ----- -------  ----------"
510 AWOUT=RHOUT/100
```

```
520 VPRES=VP1*EXP(VP2/(TEMPC+VP3))
530 KP1=PCONST*(AREACM2/10)*VPRES*TIMEINCSEC/THICKNESSM/
    SOLIDSG
540 TEXRATE=TEXRA*EXP(TEXRB*AWIN1)
550 TEXRATE=TEXRATE*EXP(ER*(1/(TEMPC+K)+TA))
560 IF STORCNT>=STORTIMEDAY OR STORCNT=0 THEN 580
570 IF DISPCNT<DISPINCDAY THEN 630
580 TEXRATEEV=INT((LOG(ABS(TEXRATE)))/2.302585093#)
590 TEXRATEMV=TEXRATE/10^TEXRATEEV
600 PRINT #Z,USING "#### #.### ##.## ###.###  +#.###E+##";
    STORCNT, AWIN1, H2ODDB*100, TEX, TEXRATEMV, TEXRATEEV
610 IF STORCNT>=STORTIMEDAY THEN 730
620 DISPCNT=0
630 DISPCNT=DISPCNT+TIMEINCDAY
640 STORCNT=STORCNT+TIMEINCDAY
650 TEX=TEX*EXP(TEXRATE*TIMEINCDAY)
660 DH2O=KP1*(AWOUT-AWIN1)
670 H2ODDB=H2ODDB+DH2O
680 AWIN2=1-EXP((H2ODDB*100-IA)/IB)
690 DAWIN=AWIN2-AWIN1
700 TEX=TEX+MEB*DAWIN
710 AWIN1=AWIN2
720 GOTO 540
730 PRINT #Z,
740 PRINT #Z,;"*****************************************"
750 IF Z=1 THEN CLOSE #1:END
760 PRINT "HARD COPY? YES,1 : NO,2"
770 INPUT Z
780 IF Z=2 THEN END
790 OPEN "lpt1:"AS #1
800 GOTO 260
810 END
```

APPENDIX D

SAMPLE COMPUTER READOUT

****

OUTSIDE %RH =	77.09
TEMP, C =	21.32
SMITH,A =	1.489
SMITH,B =	-9.087
MA =	22.35
MB =	-28.6
KA =	.001414
KB =	4.234
PRODUCT WT., G =	25.13
%MDB, G/100G =	11.82
AREA, CM2 =	318.69
Thickness, mil =	2
P,KG*M/M2*S*PA =	8.75D-16
DT, HR =	24

DAYS	AW	%MDB	TEXTURE	TEX RATE
0	0.679	11.82	3.300	+1.482E -2
7	0.689	12.11	3.363	+1.547E -2
14	0.698	12.37	3.490	+1.606E -2
21	0.706	12.61	3.682	+1.659E -2
28	0.712	12.82	3.940	+1.706E -2
35	0.718	13.00	4.268	+1.749E -2
42	0.724	13.17	4.673	+1.788E -2
49	0.728	13.32	5.163	+1.823E -2
56	0.732	13.46	5.748	+1.855E -2
63	0.736	13.59	6.440	+1.884E -2
70	0.739	13.70	7.255	+1.910E -2
77	0.742	13.80	8.210	+1.934E -2
84	0.745	13.89	9.327	+1.956E -2
91	0.747	13.98	10.629	+1.975E -2
98	0.749	14.06	12.147	+1.993E -2
105	0.751	14.13	13.914	+2.010E -2
112	0.753	14.19	15.970	+2.024E -2
119	0.754	14.25	18.361	+2.038E -2
126	0.756	14.30	21.141	+2.050E -2
130	0.757	14.33	22.928	+2.057E -2

****

BIBLIOGRAPHY

BIBLIOGRAPHY

ANON. 1975. Standard methods of testing for water vapor transfer of materials in sheet form. In: The Annual Book of ASTM Standards. Philadelphia. E-96-66.

ANON. 1981. Spritz cookie recipe. In: Better Homes and Gardens New Cook Book. Meredith Corp. Des Moines, Iowa. p.165.

Association of Official Analytical Chemists. 1980. Moisture determination method 14.002,14.003. The Association, Washington, D.C. p 211.

Axford, D.W.E., Colwell, K.H., Cornford, S.J., and Elton, G.A.H. 1968. Effect of loaf specific volume on the rate and extent of staling in bread. J. Sci. Food Agric. 19:95.

Ayer, J.E., Schmitt, D.R., and Manfield, R.M. 1960. Permeation of water vapor through polymeric films. J. Appl. Polym. Sci. 3:1.

Barrer, R.N. 1941. Diffusion in and Through Solids. Cambridge University Press, London.

Becker, H.A. and Sallans, H.R. 1956. A study of the desorption isotherms of wheat at 25 C and 50 C. Cereal Chem. 33:79.

Bettelheim, F.A. and Ehrlich, S.H. 1963. Water vapor sorption of mucopolysaccharides. J. Phys. Chem. 67:1948.

Bookwalter, G.N., Moser, H.A., Pfister, V.F., and Griffin, E.L. 1968. Storage stability of blended food products, formula No.2: a corn-soy-milk food supplement. Food Technol. 22:1581.

Bourne, M.C. 1966a. A classification of textural objective methods for measuring texture and consistency of foods. J. Food Sci. 31:1011.

Bourne, M.C. 1966b. Measurement of shear and compression components of puncture tests. J. Food Sci. 31:282.

Bourne, M.C. 1968. Texture profile of ripening pears. J. Food Sci. 33:223.

Brunauer, S., Emmett, P.H., and Teller, E. 1938. Adsorption of gases in multi-molecular layer. J. Am. Chem. Soc. 60:309.

Bruns, A.J., and Bourne, M.C. 1975. Effects of sample dimensions on the snapping force of crisp foods. J. Texture Studies. 6:445-458.

Chirife, J., Boquet, R., and Iglesias, H.A. 1979. The mathematical description of water sorption isotherm of foods in the high range of water activity. Lebensm. Wiss. Technol. 12(3):150.

Doty, P.M., Aiken, W.H., and Mark, H. 1946. Temperature dependence of water vapor permeability. Ind. Engng. Chem. 38:788.

Flood, E.A. and Farhan, F.M. 1963. Stresses and strains in adsorbate-adsorbent systems V: thermodynamic theory of adsorption-extension phenomenon. Can. J. Chem. 41:1703.

Friedman, H.H., Whitney, J.E., and Szczesniak, A.S. 1963. The texturometer - a new instrument for objective texture measurement. J. Food Sci. 28:390.

Fritsch, C.W. and Gale, J.A. 1977. Hexanal as a measure of rancidity in low fat foods. J. Am. Oil Chem. Soc. 54:225.

Hauser, P.M., and McLaren, A.D. 1948. Permeation through and sorption of water vapor by high polymers. Ind. Engng. Chem. 40:112.

Heldman, D.R. 1974. Computer simulation of vitamin stability in foods. Paper presented at seminar on stability of vitamins in food for the Association of Vitamin Chemists, Chicago, IL.

Hendel, C.E., Silveira, V.G. and Harrington, W.O. 1955. Rates of nonenzymatic browning of white potato during dehydration. Food Tech. 9:433-438.

Kapsalis, J., Drake, B., and Johansson, B. 1970. Textural Properties of Dehydrated Foods Relationships with the thermodynamics of water vapor sorption. J. Texture Studies. 1:285.

Kapsalis, J.G., Walker, J.E., and Wolf, W. 1970. A physico-chemical study of the mechanical properties of low and intermediate moisture foods. J. Texture Studies. 1:464-483.

Kim, S.K. and D'Appolonia, B.L. 1977a. Bread staling studies: I. Effect of protein content on staling rate and bread crumb pasting properties. Cereal Chem. 54:207.

Kim, S.K. and D'Appolonia, B.L. 1977b. Bread staling studies: II. Effect of protein content and storage temperature on the role of starch. Cereal Chem. 54:216.

Kramer, A. 1955. Food quality and quality control; Chapter 23 in: Handbook of Food and Agriculture. Reinhold Publ. Co., New York. p. 733.

Kramer, A. 1964. Definition of texture and its measurement in vegetable products. Food Technol. 18:304.

Kulp, K. and M. Olewnik. 1984. Starch functionality in cookie systems. paper presented at 69th Annual Meeting of American Association of Cereal Chemists. Minneapolis, MN.

Kuntz, I.D. Jr. and Kauzmann, W. 1974. Hydration of proteins and polypeptides. Adv. in Protein Chemistry. 22:239.

Kwolek, W.F., and Bookwalter, G.N. 1971. Predicting storage stability from time-temperature data. Food Technol. 25:1025.

Labuza, T.P. 1971. Properties of water as related to the keeping quality of foods. Proc. 3rd Int'l Congress, Institute of Food Technologists, p. 618.

Labuza, T.P. 1974. Storage stability and improvement of intermediate moisture foods phase II. Tech. Rept. N75-18900. NTIS, U.S. Dept. of Commerce. Springfield, Va.

Labuza, T.P. and Bergquist, S. 1983. Kinetics of oxidation of potato chips under constant temperature and sine wave temperature conditions. J. Food Sci. 48:712-715.

Labuza, T.P. and Kamman, J.F. 1983. Reaction kinetics and accelerated tests simulation as a function of temperature. In: Saguy (Ed.) Computer-Aided Techniques in Food Technology. Marcel Dekker, New York. 71-115.

Labuza, T.P., McNally, L., Gallagher, D., Hawkes, J., and Hurtado, F. 1972. Stability of =intermediate moisture foods. I. Lipid oxidation. J. Food Sci. 37:154-159.

Lakhanpal, M.L. and Flood, E.A. 1957. Stresses and strains in adsorbate-adsorbent systems IV: contractions of activated carbon on adsorption of gases and vapors at low initial pressures. Can. J. Chem. 35:887.

Lang, K.W. and Steinberg, M.P. 1980. Calculation of moisture content of a formulated food system to any given water activity. J. Food Sci. 45:228.

Lang, K.W. and Steinberg, M.P. 1981. Predicting water activity from 0.30 to 0.95 of a multicomponent food formulation. J. Food Sci. 46(3):670.

Langmuir, I. 1918. The adsorption of gases on plane surface of glass, mica and platinum. J. Am. Chem. Soc. 40:1361

Lund, D.B. 1982. Quantifying reactions influencing quality of foods: texture,flavor, and appearance. J. Food Proc. Pres. 6:133-153.

Lund, D.B. 1983. Kinetics of Physical Changes in Foods. Presented at 1983 Winter Meeting of ASAE.

Lundgren, H.P. 1967. Wool structure modified for greater durability: some considerations of requirements. Proceedings Symp. Fibrous Proteins, Australia.

Madsen, Donald H. Psychrometric Properties. HP-67 Users' Library Program 867D.

Martinez, F. and Labuza, T.P. 1968. Rate of deterioration of freeze-dried salmon as a function of relative humidity. J. Food Sci. 33:241.

Masuzawa, M. and Sterling, C. 1968. Gel-Water relationships in hydrophilic polymers: thermodynamics of sorption of water vapor. J. Applied Polymer Sci. 12:2023.

Meisner, D.F. 1953. Importance of temperature and humidity in the transportation and storage of bread. Baker's Dig. 27:109.

Mizrahi, S., and Karel, M. 1978 Evaluation of kinetic model for reactions in moisture-sensitive products using dynamic storage conditions. J. Food Sci. 43:749.

Mizrahi, S., Labuza, T.P. and Karel, M. 1970. Computer-aided predictions of extent of browning in dehydrated cabbage. J. Food Sci. 35:799.

Mohsenin, N.N. 1970a. Physical Properties of Plant and Animal Materials, Volume I - Structural, physical characteristics and mechanical properties. Gordon and Breach Science Publishers, New York. p. 743.

Mohsenin, N.N. 1970b. Application of engineering techniques to evaluation of texture of solid food materials. J. Texture Studies. 1:133.

Myers, A.W., Myer, J.A., Rogers, C.E., Stannett, V., and Szwarc, M. 1961. Studies in the gas and vapor permeability of plastic films and coated papers. Part VI. The permeation of water vapor. T.A.P.P.I. 44:1961.

Paul, P.C., and Palmer, H.H. 1972. Food Theory and Applications. John Wiley and Sons, Inc. 174-175.

Pence, J.W. and Standbridge, N.N. 1955. Effects of storage temperature and freezing on the firming of a commercial bread. Cereal Chem. 32:519.

Perry, Robert H. ed. 1973. Chemical Engineers Handbook Fifth Edition. McGraw-Hill Book Company, New York,NY. p. 17-35.

Purwadaria, H.K. 1977. Computer simulation of vitamin dehydration in a dry model food system during storage. M.S. Thesis, Dept. of Food Science and Human Nutrition, Michigan State University, E. Lansing, MI.

Purwadaria, H.K., Heldman, D.R., and Kirk, J.R. 1979. Computer simulation of vitamin degradation in a dry model food system during storage. J. Food Proc. Engr. 3:7.

Quast, D.G., and Karel, M. 1972. Computer simulation of storage life on foods undergoing spoilage by two interacting mechanisms. J. Food Sci 37:679.

Quast, D.G. and Karel, M. 1973. Simulation shelf life. Modern Pack. 3:50.

Quast, D.G., Karel, M. and Rand, W.M. 1972a. Effects of environmental factors on the oxidation of potato chips. J. Food Sci. 37:584.

Quast, D.G., Karel, M., and Rand, W.M. 1972b. Development of a mathematical model for oxidation of potato chips as a function of oxygen pressure, extent of oxidation and equilibration relative humidity. J. Food Sci. 37:673.

Ragnarsson, J.O. and Labuza, T.P. 1977. Accelerated shelf-life testing for oxidative rancidity in foods. Food Chem. 2:291.

Ragnarsson, J.O., Leick, D. and Labuza, T.P. 1977. Accelerated temperature study of antioxidants. J. Food Sci. 42:536.

Reidy, G.A. and Heldman, D.R. 1972. Prediction of texture profile for freeze-dried foods using engineering parameters. Proc. IV. Int. Cong. Food Sci. and Technol. Vol. II. p. 198-207.

Reidy, G.A. and Heldman, D.R. 1974. Measurement of texture parameters of freeze-dried beef. J. Texture Studies. 218-226.

Rowan, J.H. 1956. Moisture permeability of glove materials for controlled atmosphere boxes. Analyt. Chem. 28:402.

Sherman, P. 1969. A texture profile of foodstuffs based on well-defined rheological properties. J. Food Sci. 34:458.

Simon, I.B., Labuza, T.P., and Karel, M. 1971. Computer aided prediction of food storage stability and oxidative deterioration of a shrimp product. J Food Sci. 36:280.

Smith, H.R. 1947a. Objective measurements of quality change in foods. Food Technol. 1:345.

Smith, S.E. 1947b. The sorption of water vapor by high polymers. J. Am. Chem. Soc. 69:646.

Szczesniak,A.S. 1963a. Objective measurement of food texture. J. Food Sci. 28:410.

Szczesniak, A.S. 1963b. Classification of textural characteristics. J. Food Sci. 28:385.

Szczesniak, A.S. 1973. Instrumental Methods of Foods: In Texture Measurement of Foods. D. Reidel Publishing Co. Boston, MA. p. 71.

Taylor, R.L., Herrmann, D.B., and Demp, A.R. 1936. Diffusion of water through insulating materials. Ind Engng. Chem. 28:1255.

Young, J.H. 1976. Evaluation of models to describe sorption and desorption equilibrium moisture content isotherms of Virginia-type peanuts. Trans. of ASAE. 146.

Zabik, M.E., Fierke, S.G., and Bristol, D.K. 1979. Humidity effects on textural characteristics of sugar-snap cookies. Cereal Chem. 56:29-33.